UiO : Department of Mathematics
University of Oslo

Environmental contours

Karoline Eskeland

Master's Thesis, Spring 2017

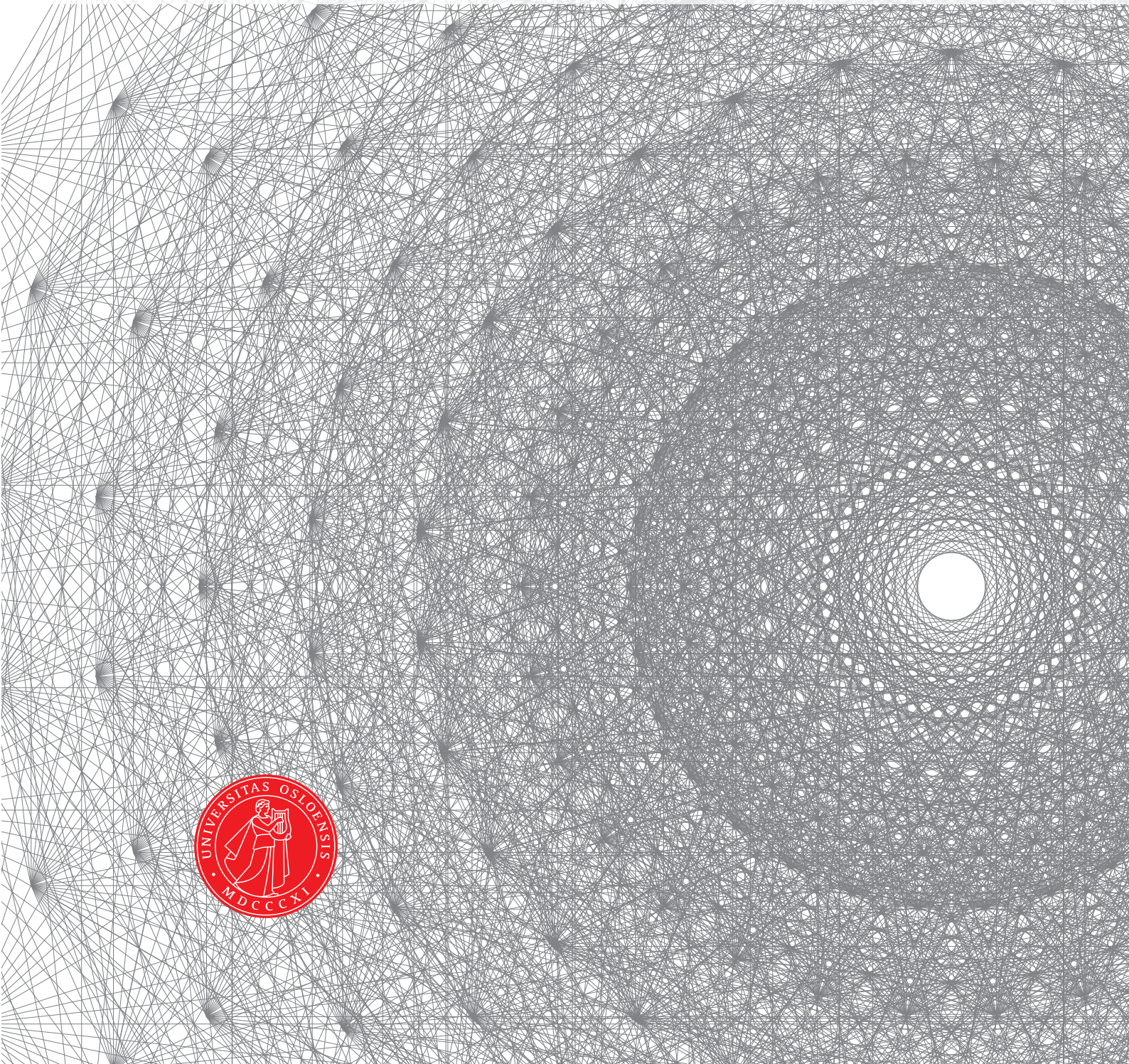

This master's thesis is submitted under the master's programme *Modelling and Data Analysis*, with programme option *Finance, Insurance and Risk*, at the Department of Mathematics, University of Oslo. The scope of the thesis is 60 credits.

The front page depicts a section of the root system of the exceptional Lie group E_8, projected into the plane. Lie groups were invented by the Norwegian mathematician Sophus Lie (1842–1899) to express symmetries in differential equations and today they play a central role in various parts of mathematics.

Abstract

Environmental contours are used as a basis for e.g., ship designs. The traditional approach to environmental contours is based on the well-known Rosenblatt transformation. However, due to the effects of this transformation the probabilistic properties of the resulting environmental contour can be difficult to interpret. An alternative approach to environmental contours uses Monte Carlo simulations on the joint environmental model, and thus obtain a contour without the need for the Rosenblatt transformation. This contour have well-defined probabilistic properties, but may sometimes be overly conservative in certain areas. In this paper we give a precise definition of the concept of the exceedance probability which is valid for all types of environmental contours. Moreover, we show how to estimate the exceedance probability of a given environmental contour, and use this to compare different approaches to contour constructions. The methods are illustrated by numerical examples based on real-life data.

For comparison of environmental contours and finding the best contour for the given application, we have also included a third type of environmental contours, the Iso contours. We adjust the contours so that they get the same desired exceedance probability, which makes it possible to compare the contours graphically. We find that the best contour is the one with the lowest area as we want as little requirements for the construction of the design as possible as well as we want it to be as little conservative as possible.

Acknowledgements

I would like to thank Arne Bang Huseby for being a great supervisor and making time when needed throug the entire time of writing this master thesis. I would also like to thank my co-supervisor, Erik Vanem, for the interesting examples we have been working further on.

This paper has been written with support from the Research Council of Norway (RCN) through the project *ECSADES* Environmental Contours for Safe Design of Ships and other marine structures. I will thank the manager of this project for letting me be a part of it, and even participate in meetings in Aberdeen, at Høvik in Oslo, and the upcoming conference in Slovenia in June 2017.

I have learned a lot during the time of writing this master thesis, and I am grateful for all the support from fellow students, friends and family.

Karoline Eskeland
Blindern, May 2017

Contents

1 INTRODUCTION

Environmental contours are widely used as a basis for e.g., ship design. Such contours allow the designer to verify that a given mechanical structure is safe, i.e, that the failure probability is below a certain value. A realistic model of the environmental loads and the resulting response is crucial for structural reliability analysis of mechanical constructions exposed to environmental forces. See [Win+93] and [HW09]. For applications of environmental contours in marine structural design, see e.g., [BHØ10], [Fon+13], [JEF11], [Moa09] and [Dit02].

The traditional approach to environmental contours is based on the well-known *Rosenblatt transformation* introduced in [Ros52]. This transformation maps the environmental variables into independent standard normal variables. Using the transformed environmental variables a contour with the desired properties can easily be constructed by identifying a sphere centered in the origin and with a suitable radius. More specifically, the sphere can be chosen so that any non-overlapping convex failure region has a probability less than or equal to a desired exceedence probability. The corresponding environmental contour in the original space can then be found by transforming the sphere back into the original space.

However, a convex region in the transformed space does not necessarily correspond to a convex region in the original space. Thus, the properties of the resulting environmental contour are difficult to interpret. To avoid such problems, contours in the original space can be constructed by using Monte Carlo simulations on the joint environmental model. See [HVN13], [HVN15b] and [HVN15a]. By using this methodology, every calculation is carried out in the original environmental space, and thus the use of the Rosenblatt transformation is avoided. For simplicity we refer to the contours obtained by this approach as Monte Carlo contours. Contours constructed using the suggested Monte Carlo simulation approach will always be convex sets. This yields a more straightforward interpretation of the contours. Another advantage of this approach is a more flexible framework for establishing environmental contours, which for example simplifies the inclusion of effects such as future projections of the wave climate related to climatic change. See [VB12]. It should be noted, however, that convex contours may not fit the joint distributions of the environmental variables well. Thus, this limitation may sometimes be too restrictive.

In this paper we will give a precise definition of the concept of exceedence probability which is valid for all types of environmental contours. Moreover, we show how to estimate the exceedence probability of a given environmental contour, and use this to compare different approaches to contour construction. The methods are illustrated using the examples introduced in [VB15].

In the last section, *the inverse problem*, we compare contours with the same desired exceedance probability and we will therefore include a third type of environmental contours, the Iso contours. Such contours are determined by identifying all points where the joint density of the enviromental variables is equal to a given value. In the section of the inverse problem we will adjust the Rosenblatt contours and the Iso contours such that they get the same desired exceedance probability. The Monte Carlo contours basically has the desired exceedance probability, so these contours are not to be adjusted for comparison.

2 BASIC CONCEPTS AND RESULTS

In this paper we consider cases where the environmental conditions can be described by a vector of environmental variables, $(T, H) \in \mathbb{R}^2$, where T is the time period, and H is the wave height. An *environmental contour* is then defined as the boundary of a set $\mathcal{B} \subseteq \mathbb{R}^2$, and denoted $\partial\mathcal{B}$.

A given mechanical structure can withstand environmental stress up to a certain level. The *failure region* of the structure is the set of states of the environmental variables that imply that the structure fails. The exact shape of the failure region of a structure may be unknown. Still it may be possible to argue that the failure region belongs to a certain family which we denote by $\mathcal{E}$. A given environmental contour $\partial\mathcal{B}$ will be evaluated with respect to this family. The family $\mathcal{E}$ is chosen relative to $\mathcal{B}$ in such a way that $\mathcal{F} \cap \mathcal{B} \subseteq \partial\mathcal{B}$ for all $\mathcal{F} \in \mathcal{E}$. Thus, a failure region $\mathcal{F}$ may intersect with the boundary of $\mathcal{B}$ but not the interior of $\mathcal{B}$. The *exceedence probability* of $\mathcal{B}$ with respect to $\mathcal{E}$ is defined as:

$$P_e(\mathcal{B}, \mathcal{E}) = \sup\{P[(T, H) \in \mathcal{F}] : \mathcal{F} \in \mathcal{E}\}.$$

We observe that the exceedence probability defined above represents an upper bound on the failure probability of the structure assuming that the true failure region is a member of the family $\mathcal{E}$. Of particular interest are cases where one can argue that the failure region of a structure is *convex*. That is, cases where $\mathcal{E}$ is the class of all convex sets which do not intersect with the interior of $\mathcal{B}$. We denote the interior of $\mathcal{B}$ by $\mathcal{B}_o$.

2.1 *Maximal failure regions*

A failure region $\mathcal{F} \in \mathcal{E}$ is said to be *maximal* if there does not exist a region $\mathcal{F}' \in \mathcal{E}$ such that $\mathcal{F} \subset \mathcal{F}'$. The family of maximal regions in $\mathcal{E}$ is denoted by $\mathcal{E}^*$. If $\mathcal{F}_1, \mathcal{F}_2 \in \mathcal{E}$ and $\mathcal{F}_1 \subseteq \mathcal{F}_2$, we obviously have:

$$P[(T, H) \in \mathcal{F}_1] \leq P[(T, H) \in \mathcal{F}_2].$$

From this it follows that:

$$P_e(\mathcal{B}, \mathcal{E}) = \sup\{P[(T, H) \in \mathcal{F}] : \mathcal{F} \in \mathcal{E}^*\}.$$

This simple observation sometimes simplifies the calculation of $P_e(\mathcal{B}, \mathcal{E})$.

In order to explain this in further detail, we need the concept of a *supporting hyperplane* of a set. If Π is a hyperplane in $\mathbb{R}^n$, we let Π^- and Π^+ denote the two half-spaces bounded by the hyperplane Π. In general a supporting hyperplane of a set $\mathcal{S} \in \mathbb{R}^n$, is a hyperplane Π such that we either have $\mathcal{S} \subseteq \Pi^-$ or $\mathcal{S} \subseteq \Pi^+$, and such that $\mathcal{S} \cap \Pi \neq \emptyset$. In particular, if $\mathcal{S} \subseteq \Pi^-$, we say that Π^+ is a *supporting half-space* of $\mathcal{S}$. We observe that if Π^+ is a supporting half-space of $\mathcal{S}$, we have that $\Pi^+ \cap S \subseteq \partial\mathcal{S}$.

We then consider a case where the set $\mathcal{B}$ is convex, where all sets in the family $\mathcal{E}$ are convex as well, and let $\mathcal{F} \in \mathcal{E}$. Then it follows by standard convexity theory, that there exists a supporting hyperplane Π of $\mathcal{B}$ such that $\mathcal{B} \subseteq \Pi^-$ and $\mathcal{F} \subseteq \Pi^+$. Moreover, since $\Pi^+ \cap \mathcal{B} \subseteq \partial\mathcal{B}$, and since every half-space is convex, it follows by the definition of $\mathcal{E}$ that $\Pi^+ \in \mathcal{E}$. We have illustrated this in Figure 1.

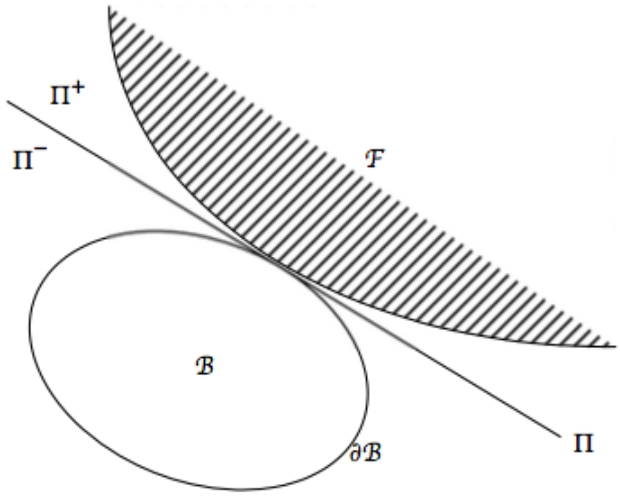

Figure 1: Illustration of the supporting hyperplane Π of $\mathcal{B}$.

Assume then that $\mathcal{F} \in \mathcal{E}^*$. If this is the case, we cannot have $\mathcal{F} \subset \Pi^+$. Hence, the only possibility is that $\mathcal{F} = \Pi^+$. Thus, we have shown that every maximal failure region $\mathcal{F}$ is a supporting half-space of $\mathcal{B}$. Conversely, we have that if Π^+ is a supporting half-space of $\mathcal{B}$, then we cannot find another supporting half-space Π'^+ such that $\Pi^+ \subset \Pi'^+$. Hence, if Π^+ is a supporting half-space of $\mathcal{B}$, then $\Pi^+ \in \mathcal{E}^*$.

We let $\mathcal{P}(\mathcal{B})$ denote the family of supporting half-spaces of $\mathcal{B}$. Then we may summarize the above discussion as follows:

Proposition 2.1 *Assume that $\mathcal{B}$ is convex and that $\mathcal{E}$ is a family of convex sets such that $\mathcal{F} \cap \mathcal{B} \subseteq \partial\mathcal{B}$ for all $\mathcal{F} \in \mathcal{E}$. Then $\mathcal{E}^* = \mathcal{P}(\mathcal{B})$. Moreover, we have:*

$$P_e(\mathcal{B}, \mathcal{E}) = \sup\{P[(T, H) \in \Pi^+] : \Pi^+ \in \mathcal{P}(\mathcal{B})\}.$$

2.2 *Transformed contours*

In this subsection we review the traditional approach to environmental contours based on the well-known Rosenblatt transformation in the context of an exceedence probability defined relative to a family of failure regions. The Rosenblatt transformation, denoted Ψ, is such that if $(T', H') = \Psi(T, H)$, then T' and H' are independent standard normally distributed. See [Hav87].

The contour for the transformed vector (T', H') is constructed as follows: Let $P_e < 0.5$ be the desired exceedence probability, and let $r > 0$ denote the $(1 - P_e)$-percentile in the standard normal distribution. We then introduce the set $\mathcal{B}'$, a circle centered at the origin and with radius r, and let $\mathcal{E}'$ be the family of all convex sets $\mathcal{F}'$ such that $\mathcal{F}' \cap \mathcal{B}' \subseteq \partial\mathcal{B}'$. By Proposition 2.1, we then have that $\mathcal{E}'^* = \mathcal{P}(\mathcal{B}')$. We then choose an arbitrary half-space $\Pi^+ \in \mathcal{P}(\mathcal{B}')$. By the rotational symmetry property of the bivariate normal distribution of (T', H') it follows that:

$$P[(T', H') \in \Pi^+] = P[T' > r] = P_e.$$

Since this is true for all $\Pi^+ \in \mathcal{P}(\mathcal{B}')$, we then get:

$$P_e(\mathcal{B}', \mathcal{E}') = \sup\{P[(T', H') \in \Pi^+] : \Pi^+ \in \mathcal{P}(\mathcal{B}')\} = P_e.$$

We then let $\mathcal{B} = \Psi^{-1}(\mathcal{B}')$, and let $\mathcal{E}$ be given by:

$$\mathcal{E} = \{\mathcal{F} = \Psi^{-1}(\mathcal{F}') : \mathcal{F}' \in \mathcal{E}'\},$$

where Ψ^{-1} denotes the inverse Rosenblatt transformation. In practice we need to limit ourselves to transform a finite number of points evenly spread out along the border $\partial\mathcal{B}'$ over to the border $\partial\mathcal{B}$. The resulting contour $\partial\mathcal{B}$ is then obtained by connecting these points with line segments. As a result the contour $\partial\mathcal{B}$ is approximated by a polygon. In this context we have chosen to transform a total of 360 points. Thus, the resulting polygon will have 360 corners.

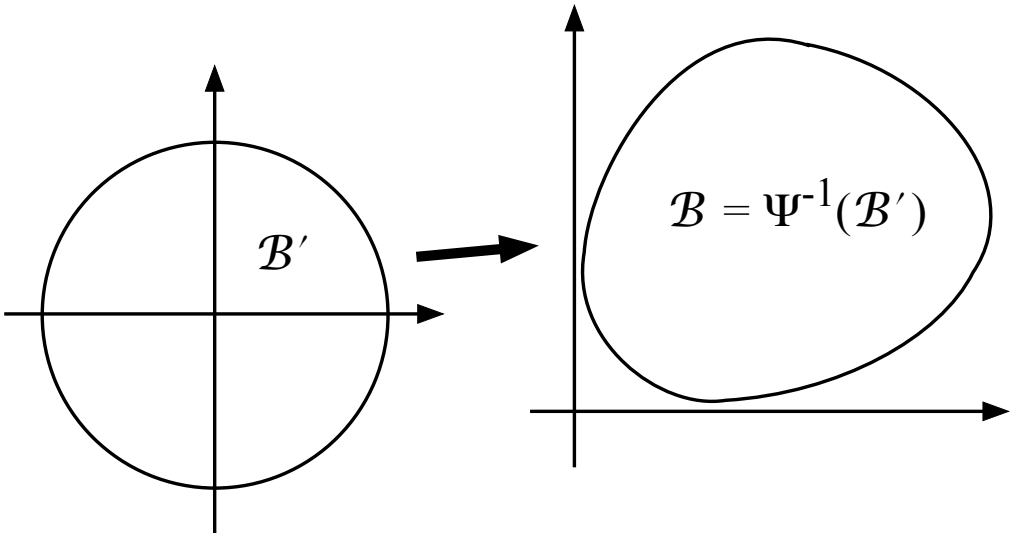

Figure 2: Obtaining the set $\mathcal{B}$ by using the inverse Rosenblatt transformation Ψ^{-1}.

In Figure 2 we have illustrated how to obtain the set $\mathcal{B}$, where the inverse mapping $\Psi^{-1}(\mathcal{M})$ of an arbitrary set $\mathcal{M}$ is defined by:

$$\Psi^{-1}(\mathcal{M}) = \{(t,h) = \Psi^{-1}(t',h') : (t',h') \in \mathcal{M}\}.$$

We then get that:

$$\begin{aligned} P_e(\mathcal{B},\mathcal{E}) &= \sup\{P[(T,H) \in \mathcal{F}] : \mathcal{F} \in \mathcal{E}\} \\ &= \sup\{P[(T,H) \in \Psi^{-1}(\mathcal{F}')] : \mathcal{F}' \in \mathcal{E}'\} \\ &= \sup\{P[(T',H') \in \mathcal{F}'] : \mathcal{F}' \in \mathcal{E}'\} \\ &= \sup\{P[(T',H') \in \Pi^+] : \Pi^+ \in \mathcal{P}(\mathcal{B}')\} = P_e. \end{aligned}$$

Thus, the contour $\partial\mathcal{B}$ has the desired exceedence probability with respect to the family $\mathcal{E}$ of failure regions.

The problem with this approach is that since $\mathcal{E}$ consists of transformed convex sets, where the transformation depends on the joint distribution of (T,H), it may be difficult to argue that a given mechanical construction should have a failure region which belongs to this particular family. In order to do so we must argue that if $\mathcal{F}$ is the true failure region for the given mechanical construction, then $\Psi(\mathcal{F})$ must be convex. It is typically much easier to argue that the true failure region $\mathcal{F}$ itself is convex, and hence avoid an argument involving the joint distributions of the environmental variables. In order to accomplish this, however, the family $\mathcal{E}$ must be redefined, and hence the exceedence probability may change.

2.3 *Convex contours*

In [HVN13], [HVN15b] and [HVN15a] the focus was restricted to contours where the set $\mathcal{B}$ itself was *convex*. Moreover, the family $\mathcal{E}$ was chosen relative to $\mathcal{B}$ as the family of all convex failure regions $\mathcal{F} \subseteq \mathbb{R}^2$ such that $\mathcal{F} \cap \mathcal{B} \subseteq \partial\mathcal{B}$. By Proposition 2.1 this makes the calculation of the exceedence probability relatively simple.

In order to briefly explain the approach we let $P_e < 0.5$ be the desired exceedence probability of $\mathcal{B}$ with resepect to $\mathcal{E}$. In order to determine $\mathcal{B}$ such that $P_e(\mathcal{B}, \mathcal{E}) = P_e$, we start out by introducing the function $C(\theta)$ defined for $\theta \in [0, 2\pi)$ as:

$$C(\theta) = \inf\{C : P[T\cos(\theta) + H\sin(\theta) > C] = P_e\}. \tag{1}$$

This means that $C(\theta)$ is the $(1 - P_e)$-percentile of the distribution of $Y(\theta) = T\cos(\theta) + H\sin(\theta)$. Furthermore, we introduce for $\theta \in [0, 2\pi)$:

$$\begin{aligned} \Pi^+(\theta) &= \{(t,h) : t\cos(\theta) + h\sin(\theta) \geq C(\theta)\}, \\ \Pi(\theta) &= \{(t,h) : t\cos(\theta) + h\sin(\theta) = C(\theta)\}, \\ \Pi^-(\theta) &= \{(t,h) : t\cos(\theta) + h\sin(\theta) \leq C(\theta)\}. \end{aligned} \tag{2}$$

By the definition of $C(\theta)$ it follows that for all $\theta \in [0, 2\pi)$ we have:

$$P[(T,H) \in \Pi^+(\theta)] = P[T\cos(\theta) + H\sin(\theta) > C(\theta)] = P_e.$$

In [HVN15b] it was shown that $\mathcal{B}$ may be expressed as:

$$\mathcal{B} = \bigcap_{\theta \in [0,2\pi)} \Pi^-(\theta),$$

assuming that $\Pi(\theta)$ intersects the boundary of $\mathcal{B}$ for all $\theta \in [0, 2\pi)$. Under this assumption it also follows that:

$$\mathcal{P}(\mathcal{B}) = \{\Pi^+(\theta) : \theta \in [0, 2\pi)\}.$$

We may then use Proposition 2.1 to compute the exceedence probability of $\mathcal{B}$ with respect to $\mathcal{E}$, and get:

$$\begin{aligned} P_e(\mathcal{B}, \mathcal{E}) &= \sup\{P[(T,H) \in \Pi^+] : \Pi^+ \in \mathcal{P}(\mathcal{B})\} \\ &= \sup\{P[(T,H) \in \Pi^+(\theta)] : \theta \in [0, 2\pi)\} \\ &= \sup_{\theta \in [0,2\pi)} P[T\cos(\theta) + H\sin(\theta) > C(\theta)] = P_e. \end{aligned}$$

We then conclude that the contour $\partial\mathcal{B}$ has the desired exceedence probability with respect to $\mathcal{E}$.

In [HVN15b] three specific methods for identifying $\partial\mathcal{B}$ are presentet, all of them using Monte Carlo simulations. In this paper we focus on the second method.

In the relevant method we assume that $C(\theta)$ in (1) is differentiable. We can then use $C(\theta)$ to identify the boundary of the set $\mathcal{B}$. For a given angle $\theta \in [0, 2\pi)$ and a small number $\delta > 0$ we consider the intersection between the two P_e-exceedance hyperplanes $\Pi(\theta)$ and $\Pi(\theta + \delta)$. From (2), this point can be found by solving the following linear equations:

$$\begin{aligned} t\cos(\theta) + h\sin(\theta) &= C(\theta), \\ t\cos(\theta + \delta) + h\sin(\theta + \delta) &= C(\theta + \delta), \end{aligned}$$

which has the following solution for t and h:

$$t = \frac{\sin(\theta+\delta)C(\theta) - \sin(\theta)C(\theta+\delta)}{\sin(\delta)},$$
$$h = \frac{-\cos(\theta+\delta)C(\theta) + \cos(\theta)C(\theta+\delta)}{\sin(\delta)}.$$

As $\delta \to 0$ the intersection point (t, h) will converge to a point in $\Pi(\theta)$ which we denote by $(t(\theta), h(\theta))$. Using l'Hôpital's rule we get that:

$$\begin{aligned}\lim_{\delta\to 0^+} t = t(\theta) &= \lim_{\delta\to 0^+} \frac{\cos(\theta+\delta)C(\theta) - \sin(\theta)C'(\theta+\delta)}{\cos(\delta)} \\ &= C(\theta)\cos(\theta) - C'(\theta)\sin(\theta),\end{aligned}$$

and

$$\begin{aligned}\lim_{\delta\to 0^+} h = h(\theta) &= \lim_{\delta\to 0^+} \frac{\sin(\theta+\delta)C(\theta) + \cos(\theta)C'(\theta+\delta)}{\cos(\delta)} \\ &= C(\theta)\sin(\theta) + C'(\theta)\cos(\theta).\end{aligned}$$

Hence, $(t(\theta), h(\theta))$ can be written as:

$$\begin{pmatrix} t(\theta) \\ h(\theta) \end{pmatrix} = \begin{bmatrix} C(\theta) & -C'(\theta) \\ C'(\theta) & C(\theta) \end{bmatrix} \cdot \begin{pmatrix} \cos(\theta) \\ \sin(\theta) \end{pmatrix},$$

where $C'(\theta)$ denotes the derivative of $C(\theta)$.

The suggested Monte Carlo method is then based on what we just did, but with the true value of the C-function and its derivative replaced by estimates. In particular, the derivative of C is found numerically by approximating C with a piecewise linear function. For more details about this, see [HVN15b]. $\partial\mathcal{B}$ is estimated by the points $(t(\theta), h(\theta))$ after inserting estimates for $C(\theta)$ and its derivative.

In order to construct the contour $\partial\mathcal{B}$, we would ideally like to calculate the point $(t(\theta), h(\theta))$ for all $\theta \in [0, 2\pi)$. However, as we did for the Rosenblatt contour, we limit the process by considering only a finite number of angles, $\theta_1 < \cdots < \theta_m$ where m is a suitable number. In our calculations we have chosen m to be 360. As a result the true contour is approximated by a polygon.

We will now explain how we estimate $C(\theta)$ by simulating from the joint distributions of T and H. In principle it is possible to simulate (T, H) by sampling directly from the joint distributions. In this context, however, we assume that this simulation is done by first simulating a vector (X, Y) from a bivariate normal distribution, and then transforming (X, Y) over to (T, H) using the inverse Rosenblatt transformation.

Assume that the vector (X, Y) is standard bivariate normally distributed, i.e, X and Y are independent and normally distributed with mean 0 and standard deviation 1. We then let:

$$R = \sqrt{X^2 + Y^2},$$
$$V = atan2(Y, X),$$

where the function $atan2(y, x)$ is described as follows:

$$atan2(y,x) = \begin{cases} \arctan(\frac{y}{x}) & \text{if } x > 0, \\ \arctan(\frac{y}{x}) + \pi & \text{if } x < 0 \text{ and } y \geq 0, \\ \arctan(\frac{y}{x}) - \pi & \text{if } x < 0 \text{ and } y < 0, \\ \frac{\pi}{2} & \text{if } x = 0 \text{ and } y > 0, \\ -\frac{\pi}{2} & \text{if } x = 0 \text{ and } y < 0, \\ \text{undefined} & \text{if } x = 0 \text{ and } y = 0. \end{cases}$$

This implies that R and V are the polar coordinates of (X, Y). It can now be shown that R and V are independent, and that $Z = R^2$ is χ^2-distributed with 2 degrees of freedom, while V becomes $R[0, 2\pi]$-distributed. This means that the density of Z is :

$$f_Z(z) = \frac{1}{2}e^{-z/2}, \quad \text{for } z > 0,$$

which is an exponential distribution with rate $\lambda = 1/2$. We then also have that $P(Z > z) = e^{-z/2}$. This means that if (X, Y) is standard bivariate normally distributed, then the probability that (X, Y) is located outside a circle with centrum in origin and with a radius r is equal to $e^{-r^2/2}$.

To simulate from the distribution of (X, Y) we can then do the following: We start by generating U and V, where $U \sim R[0, 1]$ and $V \sim R[0, 2\pi]$. We then let $Z = -2\ln(U)$. Then it is easy to show that Z gets the density f_Z. We also calculate $R = \sqrt{Z}$. Since R and V are the polar coordinates to (X, Y), we find that:

$$X = R\cos(V),$$
$$Y = R\sin(V).$$

Let then $(T, H) = \Psi^{-1}(X, Y)$, where Ψ^{-1} is the inverse Rosenblatt transformation for the joint distributions of T and H. This way (T, H) gets the correct joint distribution.

Now let $\theta \in [0, 2\pi)$, and let $S = T\cos(\theta) + H\sin(\theta)$. For a given exceedance probability P_e we wish to estimate $C(\theta)$ such that $P(S > C(\theta)) = P_e$.

By simulating (T, H) n times as explained above, and each time calculating the resulting value of S, we can estimate $C(\theta)$ by the order observator $S_{(k)}$, where k is such that:

$$1 - \frac{k}{n} = \frac{n-k}{n} \approx P_e.$$

This method works well for moderately small exceedance probabilities. However, when P_e is very small, i.e., 0.1%, we need a large number of simulations in order to obtain stable estimates. We also have that most of the simulations yields a result close to the central area of the joint distribution, and that means that very few results provide information about the contour area. Thus, in order to get a sufficiently large number of samples in the area of the contour, a huge number of simulations is needed. This can represent a challenge.

To reduce the number of simulations, there are in [HVN15a] introduced an *importance sampling* method where all samples in the central area of the joint distribution are rejected. This way it is possible to focus the estimation on the area of interest, i.e., the area close to the contour. Still one has to generate a large number of samples as part of the rejection procedure in order to end up with a sufficiently large sample of non-rejected points. In this paper we will propose an alternative sampling scheme. In this sampling scheme we avoid sampling points from the central area of the joint distribution completely, and only sample points close to the contour. This is actually easier to do when we start out by simulating (X, Y) and then transforming this vector over to (T, H).

More specifically, we start out by simulating (X, Y) from the conditional distribution for (X, Y) given that this vector falls outside a circle with radius, say r_0. The specific value of r_0 will be determined below. This corresponds to simulating (X, Y) from the conditional distribution given that $R = \sqrt{X^2 + Y^2} > r_0$, or equivalently from the conditional distribution for (X, Y) given that $Z = X^2 + Y^2 > z_0 = r_0^2$. To do this we need the conditional distribution for Z given that $Z > z_0$. For $z > z_0$ we have:

$$P(Z > z | Z > z_0) = \frac{P(Z > z \bigcap Z > z_0)}{P(Z > z_0)} = \frac{P(Z > z)}{P(Z > z_0)} = e^{-(z - z_0)/2}.$$

Hence, given that $Z > z_0$, $(Z - z_0)$ is also exponentially distributed with rate $\lambda = 1/2$. Thus, we can simulate from the conditional distribution for Z given $Z > z_0$ by generating $U \sim R[0, 1]$ and let $Z = z_0 - 2\ln(U) = r_0^2 - 2\ln(U)$. The angle V is generated from the $R[0, 2\pi]$-distribution. Finally, we calculate $R = \sqrt{Z}$, $X = R\cos(V)$ and $Y = R\sin(V)$ as earlier, and transform the resulting vector (X, Y) over to the vector (T, H) using the inverse Rosenblatt transformation.

By using this type of importance sampling technique we avoid simulating a large number of outcomes in the centre of the outcome space of the joint distribution for T and H far away from the contour we want to estimate. Instead, the simulations are focused in the area of interest on the outer edge of the outcome space where we expect that the contour is. If we do so, we need to correct for this by estimating $C(\theta)$ using an "adjusted" exceedance probability which takes into acount that we are not simulating from the true joint distributions of T and H. That is, we let $P_e' = P(S > C(\theta) | R > r_0)$ be this adjusted exceedance probability, and assume that r_0 is chosen such that the event $\{S > C(\theta)\}$ is contained in the event $\{R > r_0\}$. We can achieve this by ensuring that r_0 is not too large. Assuming that we have done so, we have:

$$P(S > C(\theta) | R > r_0) = \frac{P(S > C(\theta) \bigcap R > r_0)}{P(R > r_0)} = \frac{P(S > C(\theta))}{P(R > r_0)} = \frac{P_e}{e^{-r_0^2/2}},$$

where we have used that $P(R > r_0) = P(Z > r_0^2) = e^{-r_0^2/2}$. In other words, we have shown that:

$$P_e' = P(S > C(\theta) | R > r_0) = e^{r_0^2/2} \cdot P_e.$$

We can then simulate n times from this conditional distribution and estimate $C(\theta)$ as the order observation $S_{(k)}$, but where k is determined such that:

$$1 - \frac{k}{n} = \frac{n - k}{n} \approx P_e'.$$

To get this method to work, it is necessary to ensure that the event $\{S > C(\theta)\}$ is contained in the event $\{R > r_0\}$. Thus, we let $\mathcal{O}$ denote a circle centered in the origin with radius r_0. Then r_0 must be chosen so that the transformed set $\Psi^{-1}(\mathcal{O})$ is contained inside the contour we want to estimate. At the same time, r_0 should be chosen as large as possible to get the maximal effect of the importance sampling. Experiences has shown that we get a stable estimate by choosing $r_0 = 0.95 \cdot r$, where r is the radius we use to determine the Rosenblatt contour. See Subsection 2.2.

Big differences in the variations between the environmental variables T and H may have a significant effect on the precision of the contour estimates. See [HVN15b]. This is especially true since $C(\theta)$ is estimated only for a finite number of angles. In order to avoid these problems, it is in [HVN15b] recommened that the variables are standardized as part of the estimation procedure. Thus, we have applied bivariate standardization throughout this paper.

A problem with the suggested Monte Carlo method is that the estimated contour may have small irregularities. This issue is discussed in detail in [HVN15b]. In order to avoid this problem, we propose using the boundary of the convex hull of all the estimated points along the contour instead of the original polygon. This is done by using the well-known *Graham's algorithm*. See [Gra72] or [oRo98]. As a result all the irregularites are removed, and the area surrounded by the contour becomes a truely convex set. This method will be used in all our examples.

We will now take a closer look at the difference between the contour with the small irregularities, which we for simplicity will refer to as the uncorrected Monte Carlo method, and the boundary of the convex hull. To see the difference we have, in Figure 3, zoomed in on the same specific area of a Monte Carlo simulation represented by the two different contours.

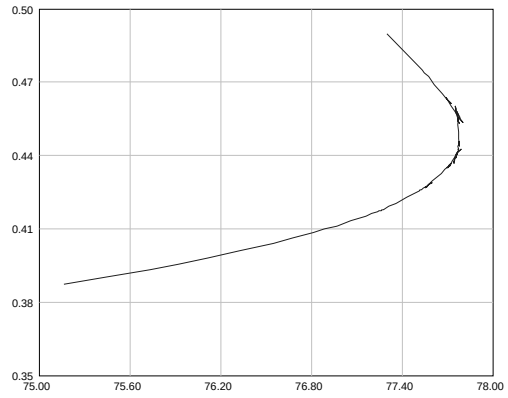

(a) The contour obtained by the uncorrected Monte Carlo method.

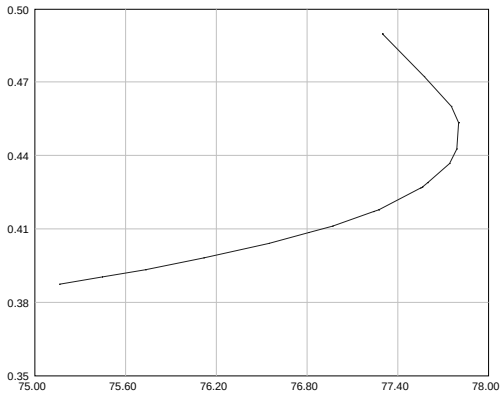

(b) The contour obtained as the boundary of the convex hull.

Figure 3: Differences between the contour obtained by the uncorrected Monte Carlo method and the contour obtained as the boundary of the convex hull.

Recall that the Monte Carlo contour is approximated by a polygon of 360 points. The polygon is constructed by drawing line segments between the points, and moving counterclockwise along the border. For the contour obtained by the uncorrected Monte Carlo method, there might be many points around the same area, and this contour includes all of them resulting in line segments back and forth. The convex hull in contrast, only includes the outlying points which means that the curls we get from the contour by the uncorrected Monte Carlo method are gone. Note, that because of the exclusion of some points, the contour obtained as the boundary of the convex hull is approximated by a polygon consisting of less than 360 points. We observe that by using the boundary of the convex hull, the contour becomes smoother than the contour obtained by the uncorrected Monte Carlo method.

To get a deeper understanding of how big the difference between these two contours is, we want to show how the angles between successive line segments vary along the border. In order to explain this further, we start with an easy example of a polygon consisting of 6 points. When moving along the polygon from point to point counterclockwise, we measure the angles between line segments illustrated by Figure 4, where the encountered angles corresponding to the corners $a, ..., f$ are marked. We observe that all the angles are positive except for the angle at corner e. Note that as we move along the border in a counterclockwise direction, positive angles results in left turns, while negative angles results in right turns. Every left turn corresponds to convexity and every right turn corresponds to concavity. We will come back to this in Section 4.

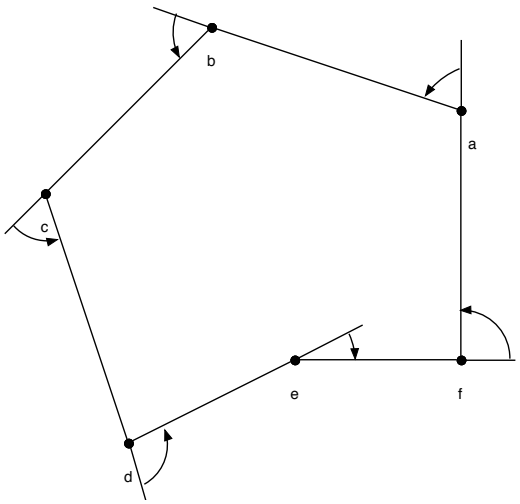

Figure 4: Measure of angles between line segments.

If we now look at the difference between the contour obtained by the uncorrected Monte Carlo method and the contour obtained as the boundary of the convex hull by looking at variations in the angles, we see a clear difference. See Figure 5.

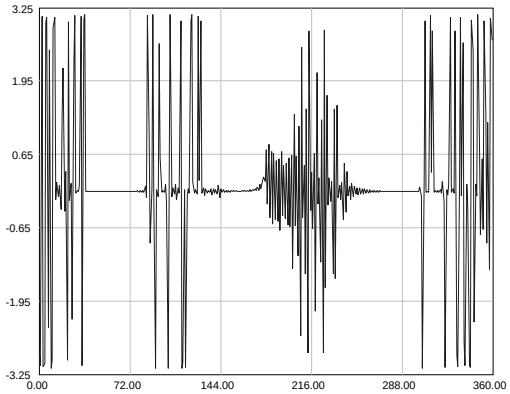

(a) Variations in angles for the contour obtained by the uncorrected Monte Carlo method.

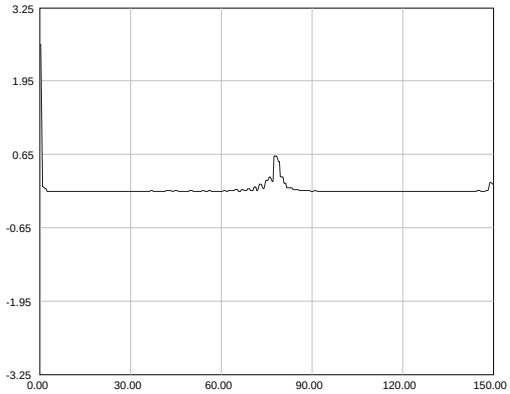

(b) Variations in the angles for the contour obtained as the boundary of the convex hull.

Figure 5: The difference between the variations in the angles between the contour obtained by the uncorrected Monte Carlo method and contour obtained as the boundary of the convex hull.

Note that the angles on the y-axis are given as radians. We observe that the contour obtained by the uncorrected Monte Carlo method consists of 360 points while the contour obtained as the boundary of the convex hull only consists of 150 points. The x-axis represents these points. Note that for the contour obtained as the boundary of the convex hull all the angles are positive, while the angles associated with the contour obtained by the uncorrected Monte Carlo method fluctuate between positive and negative numbers. However, as we can see in Figure 6, the contours will look approximatly the same zooming out on Figure 3.

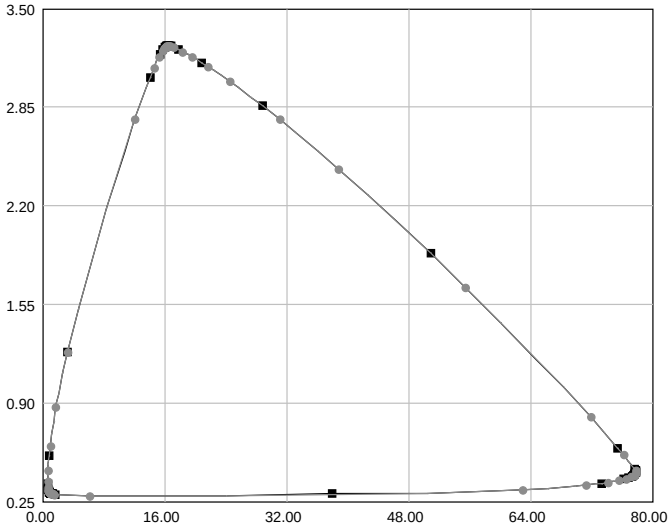

Figure 6: Black squares: Contour obtained by the uncorrected Monte Carlo method. Grey circles: Contour obtained as the boundary of the convex hull.

Contours constructed by Monte Carlo simulations have the advantage, compared to transformed contours, that it is much easier to argue that the true failure region of a given mechanical construction belongs to the family $\mathcal{E}$. The disadvantage, however, is that one is limited to convex contours. In cases where the joint distribution of (T, H) is concentrated on a non-convex area, a convex contour would typically include significant areas with very little probability mass. In such cases convex contours may lead to overly conservative designs. See [VB15].

2.4 *Iso contours*

Let the environmental variables T and H have density $f(t, h)$ and the set $\mathcal{B}$ be given by:

$$\mathcal{B} = \{(t, h) : f(t, h) \geq c\},$$

where $c > 0$ is an appropriate constant. The boundary, $\partial\mathcal{B}$, is then called an *Iso curve* or an *Iso contour* if it is given by:

$$\partial\mathcal{B} = \{(t, h) : f(t, h) = c\}.$$

In this paper we have chosen to let c be given by:

$$c = \min[f(t, h) : (t, h) \in \partial\mathcal{B}_R],$$

where $\partial\mathcal{B}_R$ denotes the Rosenblatt contour. As a result, the Iso contour is always outside of the corresponding Rosenblatt contour. This also implies that the exceedance probability of the Iso contour is always slightly less than the corresponding Rosenblatt contour. Note, however, that when we find the value of c, we only investigate a finite number of points along the Rosenblatt contour. Thus, in rare cases there may exist points on the Rosenblatt contour where the density is smaller than c. In such cases there may be points on the Iso contour which lie inside the Rosenblatt contour. In such cases the Iso contour may have an exceedance probability which is slightly larger than the corresponding Rosenblatt contour.

As for both the Rosenblatt contours and the Monte Carlo contours, the Iso contours are approximated by polygons as well.

Two main problems with Iso contours we will state in this paper is when we have:

1. Multimodal probability distributions.
2. Distributions where the contours are not closed.

When the first problem occurs, we end up with contours consisting of multiple enclosed sets. See Figure 7. The contours will then be difficult to interpret. However, all our examples are unimodal, so we will in fact not encounter this problem in this paper. We refer to [Has+17] where methods for multimodal probability distributions generates clearly defined contours.

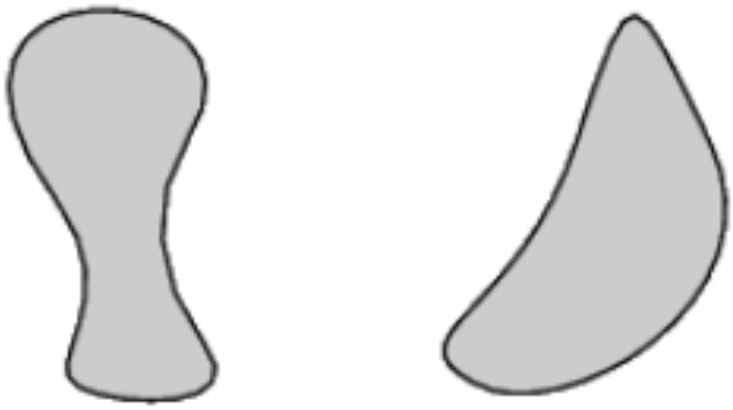

Figure 7: Example of multiple enclosed sets.

The second problem can be illustrated by a simple example. Let:

$$f(x,y) = \frac{1}{4\sqrt{xy}} \quad \text{where} \quad 0 < x \leq 1 \quad \text{and} \quad 0 < y \leq 1.$$

To find the Iso contours, we then need to solve $f(x,y) = c$:

$$\begin{aligned} f(x,y) &= c \\ \Leftrightarrow \frac{1}{4\sqrt{xy}} &= c \\ \Leftrightarrow \sqrt{xy} &= \frac{1}{4c} \\ \Leftrightarrow xy &= \frac{1}{16c^2}. \end{aligned}$$

Thus, in this case the Iso curves becomes hyperbolas, and we observe that these Iso contours are not closed. See Figure 8.

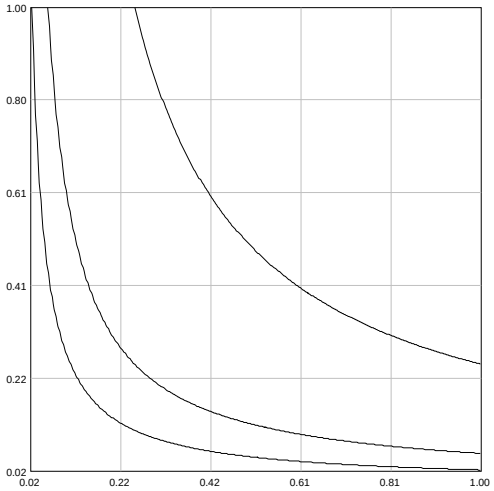

Figure 8: Iso contours for $f(x,y)$ when c=1.5, c=1.0 and c=0.5.

2.5 *Joint distributions for the environmental variables T and H*

We consider joint long-term models for the environmental variables time period (or wave period), T, and wave height, H. From [VB15], a marginal distribution is fitted to the data for significant wave height and a conditional model, conditioned on the value of significant wave height, is subsequently fitted to the wave period. The joint model is then the product of these distribution functions:

$$f_{T,H}(t,h) = f_H(h) f_{T|H}(t|h). \tag{3}$$

Joint distributions have been fitted to data assuming a three-parameter Weibull distribution for the significant wave height, H, and a lognormal conditional distribution for the wave period, T. The three-parameter Weibull distribution is parameterized by a location parameter, γ, a scale parameter α, and a shape parameter β as follows:

$$f_H(h) = \frac{\beta}{\alpha}\left(\frac{h-\gamma}{\alpha}\right)^{\beta-1} e^{-[(h-\gamma)/\alpha]^\beta}, \quad h \geq \gamma. \tag{4}$$

The lognormal distribution has two parameters, the log-mean μ and the log-standard deviation σ and is expressed as:

$$f_{T|H}(t|h) = \frac{1}{t\sqrt{2\pi}} e^{-[(\ln(t)-\mu)^2/(2\sigma^2)]}, \quad t \geq 0,$$

where the dependence between H and T is modelled by letting the parameters μ and σ be expressed in terms of H as follows:

$$\mu = \mu(h) = E[\ln(T)|H=h] = a_1 + a_2 h^{a_3}, \tag{5}$$

$$\sigma = \sigma(h) = SD[\ln(T)|H=h] = b_1 + b_2 e^{b_3 h}. \tag{6}$$

The parameters $a_1, a_2, a_3, b_1, b_2, b_3$ are estimated using available data from the relevant geographical location which we will come back to in later numerical examples.

We will now describe the inverse Rosenblatt transformation for the joint model given by (3). That is, we will describe how to transform two independent standard normally distributed variables, T' and H' over to the environmental variables T and H so that these variables get their correct joint distributions.

Assume, as above, that T' and H' are independent and standard normally distributed. We denote the inverse Rosenblatt transformation by Ψ^{-1}. Expressed as coordinates, this transformation can be written as follows:

$$(T,H) = \Psi^{-1}(T',H') = (\Psi_1^{-1}(T',H'), \Psi_2^{-1}(T',H')).$$

Since the joint distributions for T and H is expressed by the marginal distribution for H and the conditional distribution for T given H, we start by describing $H = \Psi_2^{-1}(T',H')$. In this context we let G denote the cumulative distribution function for the standard normal distribution, and claim that $U = G(H')$ is uniformly distributed on the interval $[0,1]$. This is true since for $0 \leq u \leq 1$ we have that:

$$P(U \leq u) = P(G(H') \leq u) = P(H' \leq G^{-1}(u)) = G[G^{-1}(u)] = u.$$

The cumulative distribution function for U is then equal to the cumulative distribution function for the uniform distribution on the interval [0,1], which showes that U has the alleged distribution. We then let W denote the cumulative distribution function to the current three-parameter Weibull distribution, and let:

$$H = W^{-1}(U).$$

We then have that, since U is uniformly distributed on [0,1]:

$$P(H \leq h) = P(W^{-1}(U) \leq h) = P(U \leq W(h)) = W(h),$$

then H gets the correct three-parameter Weibull distribution. By taking the cumulative distribution function for the three-parameter Weibull distribution as a starter, we find that:

$$H = W^{-1}(U) = \gamma + \alpha \cdot (-\ln(U))^{1/\beta}.$$

By combining this, we get that:

$$H = \Psi_2^{-1}(T', H') = \Psi_2^{-1}(H') = \gamma + \alpha \cdot (-\ln(G(H')))^{1/\beta}.$$

To compute T, we start by compute the parameters μ and σ by (5) and (6) respectively, where we use the calculated value of H. We then find T by the formula:

$$T = e^{\sigma \cdot T' + \mu} = e^{\sigma(H) \cdot T' + \mu(H)}.$$

Combining this, we then get that:

$$T = \Psi_1^{-1}(T', H') = e^{\sigma(H) \cdot T' + \mu(H)} = e^{\sigma(\Psi_2^{-1}(H')) \cdot T' + \mu(\Psi_2^{-1}(H'))}.$$

In (4) we observe that when $0 < \beta < 1$, we also have that $1 - \beta > 0$. By taking the limit of $f_H(h)$ when $h \to \gamma^+$ we get that:

$$\begin{aligned} \lim_{h \to \gamma^+} f_H(h) &= \lim_{h \to \gamma^+} \frac{\beta}{\alpha} \left(\frac{h - \gamma}{\alpha} \right)^{\beta - 1} e^{-[(h-\gamma)/\alpha]^\beta} \\ &= \lim_{h \to \gamma^+} \frac{\beta}{\alpha} \left(\frac{\alpha}{h - \gamma} \right)^{1 - \beta} e^{-[(h-\gamma)/\alpha]^\beta} \\ &= \infty. \end{aligned} \tag{7}$$

Hence, $f_{T,H}(t, h)$ has vertical asymptote along the line where $h = \gamma$. This implies that the Iso contour is not closed. This is similar to the issue illustrated in Figure 8. In Subsection 5.3 we have two cases where this happens.

3 UPPER BOUND ON THE EXCEEDENCE PROBABILITY

In Subsection 2.1 we explained how to compute the exceedence probability of a convex set by using Proposition 2.1. In this section we approach the problem of computing the exceedence probability of a general environmental contour. More specifically we assume that $\mathcal{B} \subseteq \mathbb{R}^2$ is a *simply connected*, but not necessarily convex set. Intuitively a simply connected set is a connected set with no holes.

As in the previous section we let $\mathcal{E}$ be the family of all convex sets $\mathcal{F} \subseteq \mathbb{R}^2$ such that $\mathcal{F} \cap \mathcal{B} \subseteq \partial\mathcal{B}$. In order to verify that $\partial\mathcal{B}$ has the correct exceedence probability with respect to $\mathcal{E}$, we have to compute $P_e(\mathcal{B}, \mathcal{E})$. Since $\mathcal{B}$ does not need to be convex, we cannot assume that $\mathcal{E}^*$ is equal to $\mathcal{P}(\mathcal{B})$. This problem is illustrated in Figure 9. In this figure the set $\mathcal{B}$ is not convex. Then it is possible to find a set $\mathcal{F} \in \mathcal{E}$ which is not contained in any supporting half-space of $\mathcal{B}$. In fact any half-space containing $\mathcal{F}$ will overlap with the interior of $\mathcal{B}$ and hence cannot be a supporting half-space of $\mathcal{B}$.

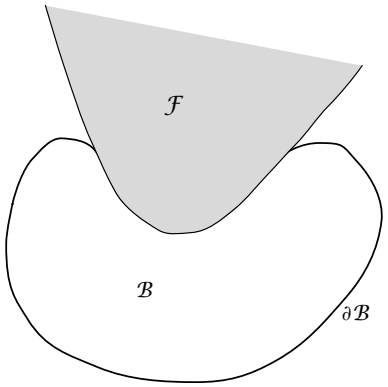

Figure 9: The convex set $\mathcal{F} \in \mathcal{E}$ is *not* contained in any supporting half-space of $\mathcal{B}$.

In order to compute $P_e(\mathcal{B}, \mathcal{E})$ for a general simply connected set we need an efficient way of identifying the family $\mathcal{E}^*$. The fact that $\mathcal{E}^*$ typically is an infinite family makes this difficult.

Instead of identifying the family $\mathcal{E}^*$ directly, it can sometimes be easier to introduce an alternative family of failure regions. We denote this family by $\tilde{\mathcal{E}}$, and assume that this family is such that for each $\mathcal{F} \in \mathcal{E}$, there exists a set $\tilde{\mathcal{F}} \in \tilde{\mathcal{E}}$ such that $\mathcal{F} \subseteq \tilde{\mathcal{F}}$. By this assumption we immediately get:

$$P_e(\mathcal{B}, \mathcal{E}) \leq P_e(\mathcal{B}, \tilde{\mathcal{E}}).$$

This means that by introducing the alternative family $\tilde{\mathcal{E}}$ and base the calculations on this, we get an upper bound on the exceedence probability.

The point here is that by choosing $\tilde{\mathcal{E}}$ in a clever way, it may be much easier to compute the upper bound on the exceedence probability.

In order to explain this in more detail, we consider a specific family $\tilde{\mathcal{E}}$. We assume that $\mathcal{B}$ is given, and as before we let $\mathcal{E}$ be the family of all convex sets $\mathcal{F} \subseteq \mathbb{R}^2$ such that $\mathcal{F} \cap \mathcal{B} \subseteq \partial\mathcal{B}$. We then choose an arbitrary convex set $\mathcal{F} \in \mathcal{E}$. Then there exists a

maximal set $\mathcal{F}^* \in \mathcal{E}$ such that $\mathcal{F} \subseteq \mathcal{F}^*$ having at least point x_0 in common with the contour $\partial\mathcal{B}$, i.e., $x_0 \in \mathcal{F}^* \cap \partial\mathcal{B}$. We then let $\Pi(x_0)$ be a hyperplane supporting $\mathcal{F}^*$ at x_0, such that $\mathcal{F}^* \subseteq \Pi^+(x_0)$, where $\Pi^+(x_0)$ is the half-space bounded by $\Pi(x_0)$ and containing $\mathcal{F}^*$. Finally, we introduce the set $\tilde{\mathcal{F}}(x_0) = \Pi^+(x_0) \setminus \mathcal{B}_o$. See Figure 10. It is then clear that $\mathcal{F} \subseteq \mathcal{F}^* \subseteq \tilde{\mathcal{F}}(x_0)$.

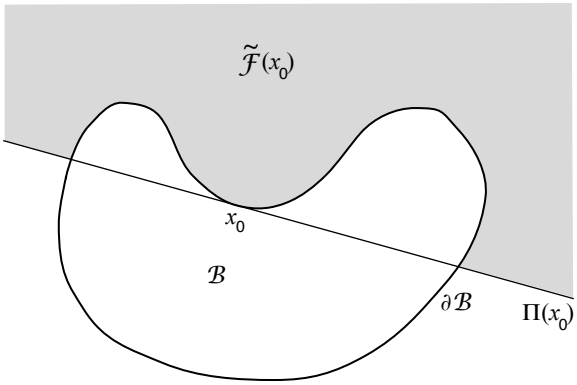

Figure 10: The construction of the set $\tilde{\mathcal{F}}(x_0)$.

The same construction can be carried out along the entire border of $\mathcal{B}$. Thus, for any $x \in \partial\mathcal{B}$ we define $\tilde{\mathcal{F}}(x)$ to be the corresponding set constructed as above by identifying a maximal set in $\mathcal{E}$ containing the point x. Moreover, we define $\tilde{\mathcal{E}} = \{\tilde{\mathcal{F}}(x) : x \in \partial B\}$. We then have that for each $\mathcal{F} \in \mathcal{E}$, there exists a set $\tilde{\mathcal{F}} \in \tilde{\mathcal{E}}$ such that $\mathcal{F} \subseteq \tilde{\mathcal{F}}$. We observe that the family $\tilde{\mathcal{E}}$ is indexed by the points in $\partial\mathcal{B}$. Thus, we may estimate $P[(T, H) \in \tilde{\mathcal{F}}(x)]$ for all $x \in \partial\mathcal{B}$ and plot the result. An upper bound on the exceedence probability, $P_e(\mathcal{B}, \mathcal{E})$, can then be found by identifying the maximum value of this function, which by definition is equal to $P_e(\mathcal{B}, \tilde{\mathcal{E}})$.

We also observe that if $\mathcal{B}$ is itself *convex*, we get that $\mathcal{E}^* = \tilde{\mathcal{E}}$. Thus, in this case the upper bound is equal to the exceedence probability of $\mathcal{B}$ with respect to $\mathcal{E}$, i.e., $P_e(\mathcal{B}, \mathcal{E}) = P_e(\mathcal{B}, \tilde{\mathcal{E}})$. On the other hand, if parts of the set $\mathcal{B}$ is strongly non-convex, as in Figure 10, the upper bound can be rather crude.

3.1 *Numerical examples*

In this subsection we illustrate the proposed method by considering numerical examples introduced in [VB15].

The parameters $a_1, a_2, a_3, b_1, b_2, b_3$ from Subsection 2.5 are estimated using available data from the relevant geographical location. In the examples considered here the parameters are fitted based on data sets from West Shetland, West of Africa - Nigeria and Northwest of Australia. We consider data for three different cases for both West Shetland and Northwest of Australia: *Total sea*, *wind sea* and *swell*, and for one case for West of Africa: *Swell*. Wind sea is defined as waves coming from local wind. Swell is defined as waves coming from wind far away or waves that keeps going after the wind has slowed down. And finally, total sea is the sum of wind sea and swell. For every locations, the parameters for the three-parameter Weibull distribution are listed in one table, while the parameters for the conditional log-normal distribution are listed in another table.

In the examples we use return periods of 25 years, 10 years and 1 year. For West Shetland and West of Africa the models are fitted using sea states representing periods of 3 hours. Thus, we get 8 data points per 24 hours. For Northwest of Australia the models are fitted using sea states representing periods of 1 hour. Thus, we get 24 data points per 24 hours.

Hence, we have the following desired exceedance probabilities:

- 25 years return period for West Shetland and West of Africa:
$$P_e = \frac{1}{25 \cdot 365.25 \cdot 8} = 1.3689 \cdot 10^{-5}.$$
- 25 years return period for Northwest of Australia:
$$P_e = \frac{1}{25 \cdot 365.25 \cdot 24} = 4.5631 \cdot 10^{-6}.$$
- 10 years return period for West Shetland and West of Africa:
$$P_e = \frac{1}{10 \cdot 365.25 \cdot 8} = 3.4223 \cdot 10^{-5}.$$
- 10 years return period for Northwest of Australia:
$$P_e = \frac{1}{10 \cdot 365.25 \cdot 24} = 1.1408 \cdot 10^{-5}.$$
- 1 year return period for West Shetland and West of Africa:
$$P_e = \frac{1}{1 \cdot 365.25 \cdot 8} = 3.4223 \cdot 10^{-4}.$$
- 1 year return period for Northwest of Australia:
$$P_e = \frac{1}{1 \cdot 365.25 \cdot 24} = 1.1408 \cdot 10^{-4}.$$

For more details about these examples we refer to [VB15].

In the following examples we will limit ourselves to environmental contours for all types of sea which are constructed using the traditional approach based on the Rosenblatt transformation, and the alternative approach based on Monte Carlo simulations. For every case, we will show the Rosenblatt contour and the Monte Carlo contour in the same plot. The corresponding upper bound on the exceedance probability, $P[(T, H) \in \tilde{\mathcal{F}}(x)]$ as a function of the point $x \in \partial\mathcal{B}$ for the Rosenblatt contour, along with the desired exceedance probability will be shown in another plot for the same cases.

In the plots of the environmental contours the x-axis represents the wave period measured in seconds (i.e., T), while the y-axis represents the significant wave heights measured in meters (i.e., H).

In the plots of $P[(T, H) \in \tilde{\mathcal{F}}(x)]$ as a function of the point $x \in \partial\mathcal{B}$, we let the point x run counterclockwise along the Rosenblatt contour. The starting point is set by a marker in the contour plots. A total of 360 points are used in each of these plots. The x-axis in these plots represents the index of these points.

In Table 7, Table 8 and Table 9 for West Shetland, West of Africa and Northwest of Australia respectively, we have listed the largest values of $P[(T, H) \in \tilde{\mathcal{F}}(x)]$, i.e., the upper bound on the exceedance probability, and for which x this value occurs for every type of sea and every return period. We have also listed the desired exceedance probabilites in the same tables.

3.1.1 *West Shetland*

Table 1: Fitted parameter for the three-parameter Weibull distribution for signifcant wave heights.

	α	β	γ
Total sea	2.259	1.285	0.701
Wind sea	2.139	1.176	0.318
Swell	2.527	1.460	0.337

Table 2: Fitted parameter for the conditional log-normal distribution for wave periods.

		$i=1$	$i=2$	$i=3$
Total sea	a_i	1.069	0.898	0.243
	b_i	0.025	0.263	-0.148
Wind sea	a_i	0.005	1.694	0.186
	b_i	0.050	0.191	-1.074
Swell	a_i	1.069	0.898	0.243
	b_i	0.025	0.263	-0.148

Total sea

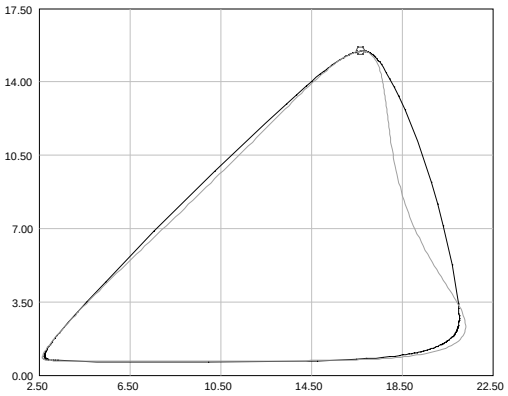

(a) Environmental contours for *total sea*, 25 years return period, constructed using the Rosenblatt transformation (grey curve) and using Monte Carlo simulation (black curve). The small marker defines the starting point of the Rosenblatt contour.

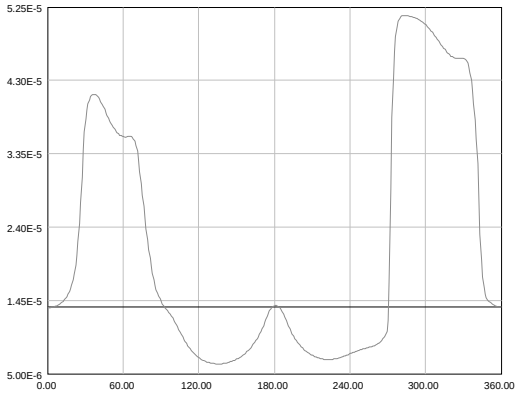

(b) $P[(T,H) \in \tilde{\mathcal{F}}(x)]$ as a function of the point $x \in \partial\mathcal{B}$ for *total sea*, 25 years return period, for the Rosenblatt contour (grey curve). The black curve represents the desired exceedence probability $P_e = 1.3689 \cdot 10^{-5}$.

Figure 11: West Shetland, total sea, 25 years return period.

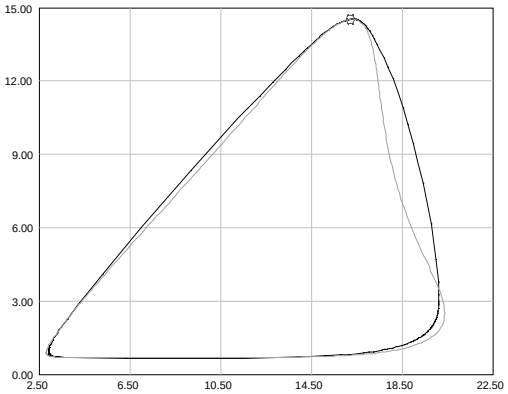

(a) Environmental contours for *total sea*, 10 years return period, constructed using the Rosenblatt transformation (grey curve) and using Monte Carlo simulation (black curve). The small marker defines the starting point of the Rosenblatt contour.

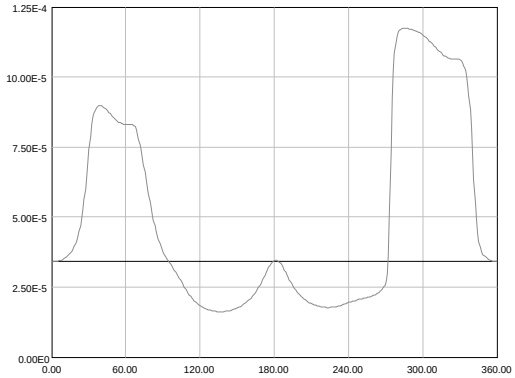

(b) $P[(T,H) \in \tilde{\mathcal{F}}(x)]$ as a function of the point $x \in \partial\mathcal{B}$ for *total sea*, 10 years return period, for the Rosenblatt contour (grey curve). The black curve represents the desired exceedence probability $P_e = 3.4223 \cdot 10^{-5}$.

Figure 12: West Shetland, total sea, 10 years return period.

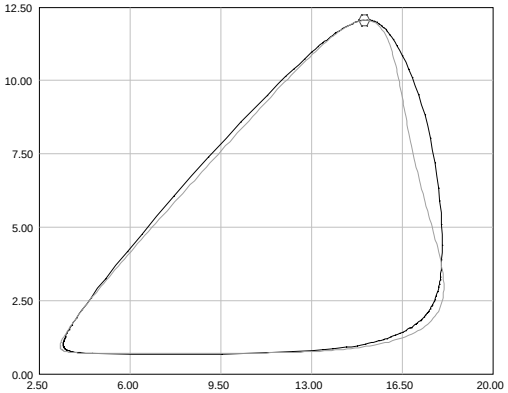

(a) Environmental contours for *total sea*, 1 year return period, constructed using the Rosenblatt transformation (grey curve) and using Monte Carlo simulation (black curve). The small marker defines the starting point of the Rosenblatt contour.

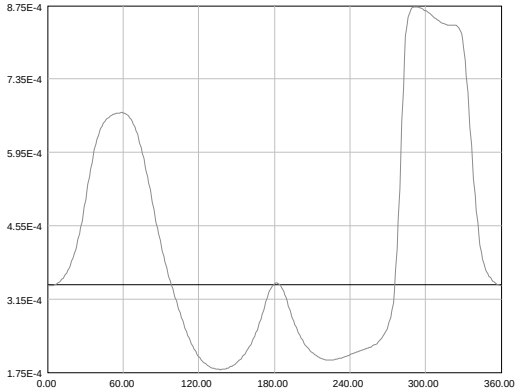

(b) $P[(T,H) \in \tilde{\mathcal{F}}(x)]$ as a function of the point $x \in \partial\mathcal{B}$ for *total sea*, 1 year return period, for the Rosenblatt contour (grey curve). The black curve represents the desired exceedence probability $P_e = 3.4223 \cdot 10^{-4}$.

Figure 13: West Shetland, total sea, 1 year return period.

Wind sea

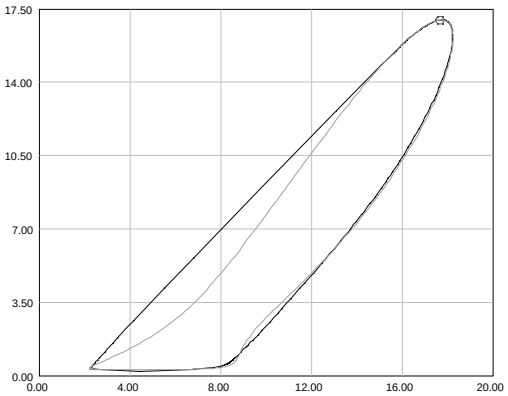

(a) Environmental contours for *wind sea*, 25 years return period, constructed using the Rosenblatt transformation (grey curve) and using Monte Carlo simulation (black curve). The small marker defines the starting point of the Rosenblatt contour.

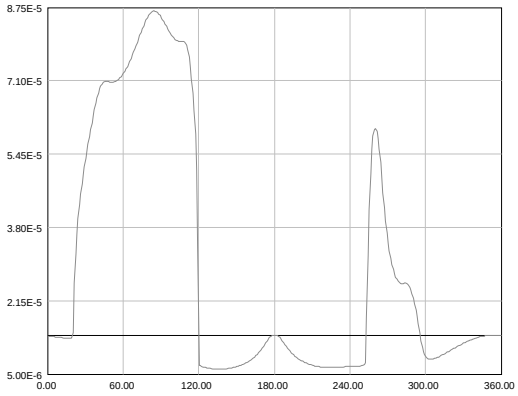

(b) $P[(T,H) \in \tilde{\mathcal{F}}(x)]$ as a function of the point $x \in \partial\mathcal{B}$ for *wind sea*, 25 years return period, for the Rosenblatt contour (grey curve). The black curve represents the desired exceedence probability $P_e = 1.3689 \cdot 10^{-5}$.

Figure 14: West Shetland, wind sea, 25 years return period.

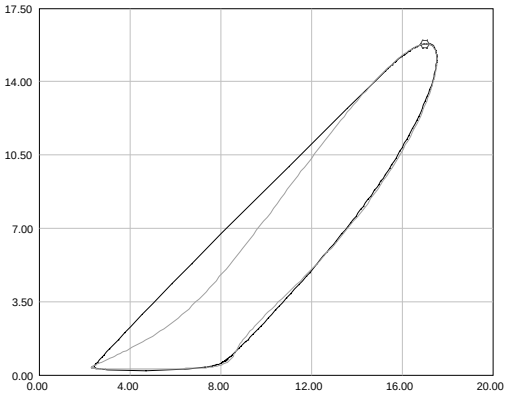

(a) Environmental contours for *wind sea*, 10 years return period, constructed using the Rosenblatt transformation (grey curve) and using Monte Carlo simulation (black curve). The small marker defines the starting point of the Rosenblatt contour.

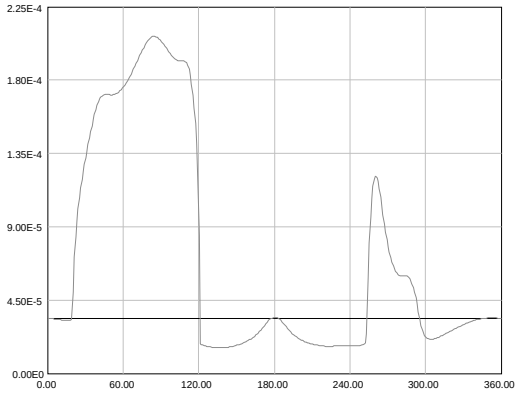

(b) $P[(T,H) \in \tilde{\mathcal{F}}(x)]$ as a function of the point $x \in \partial\mathcal{B}$ for *wind sea*, 10 years return period, for the Rosenblatt contour (grey curve). The black curve represents the desired exceedence probability $P_e = 3.4223 \cdot 10^{-5}$.

Figure 15: West Shetland, wind sea, 10 years return period.

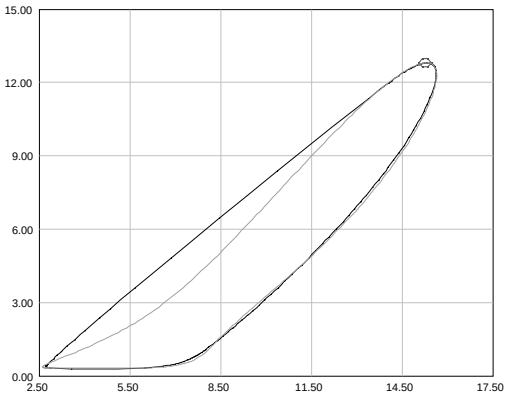

(a) Environmental contours for *wind sea*, 1 year return period, constructed using the Rosenblatt transformation (grey curve) and using Monte Carlo simulation (black curve). The small marker defines the starting point of the Rosenblatt contour.

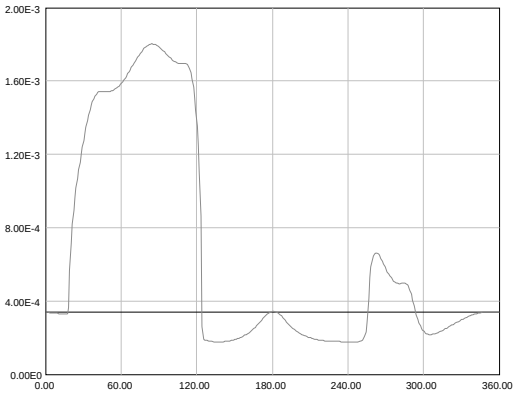

(b) $P[(T,H) \in \tilde{\mathcal{F}}(x)]$ as a function of the point $x \in \partial\mathcal{B}$ for *wind sea*, 1 year return period, for the Rosenblatt contour (grey curve). The black curve represents the desired exceedence probability $P_e = 3.4223 \cdot 10^{-4}$.

Figure 16: West Shetland, wind sea, 1 year return period.

Swell

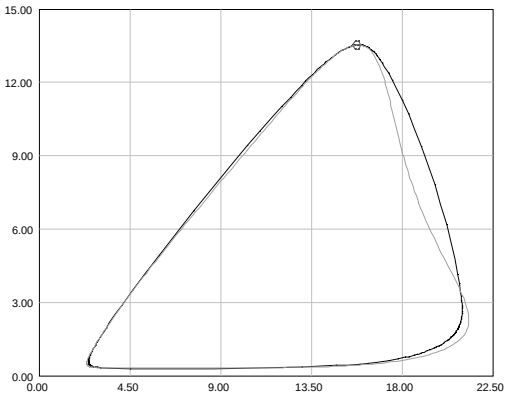

(a) Environmental contours for *swell*, 25 years return period, constructed using the Rosenblatt transformation (grey curve) and using Monte Carlo simulation (black curve). The small marker defines the starting point of the Rosenblatt contour.

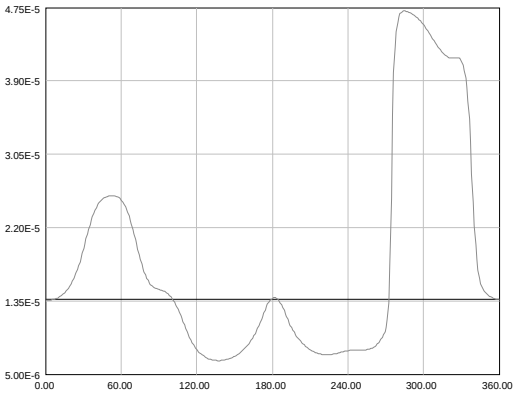

(b) $P[(T,H) \in \tilde{\mathcal{F}}(x)]$ as a function of the point $x \in \partial\mathcal{B}$ for *swell*, 25 years return period, for the Rosenblatt contour (grey curve). The black curve represents the desired exceedence probability $P_e = 1.3689 \cdot 10^{-5}$.

Figure 17: West Shetland, swell, 25 years return period.

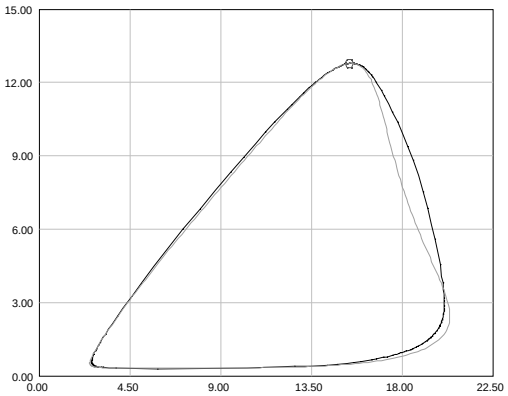

(a) Environmental contours for *swell*, 10 years return period, constructed using the Rosenblatt transformation (grey curve) and using Monte Carlo simulation (black curve). The small marker defines the starting point of the Rosenblatt contour.

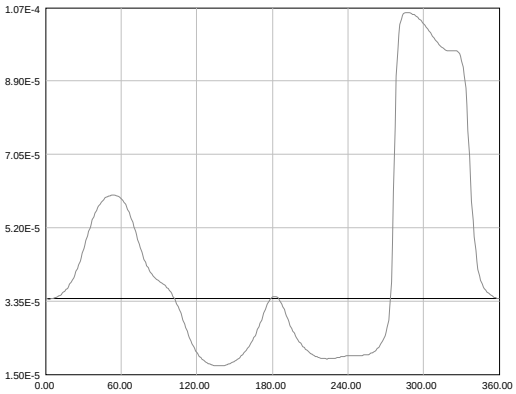

(b) $P[(T,H) \in \tilde{\mathcal{F}}(x)]$ as a function of the point $x \in \partial\mathcal{B}$ for *swell*, 10 years return period, for the Rosenblatt contour (grey curve). The black curve represents the desired exceedence probability $P_e = 3.4223 \cdot 10^{-5}$.

Figure 18: West Shetland, swell, 10 years return period.

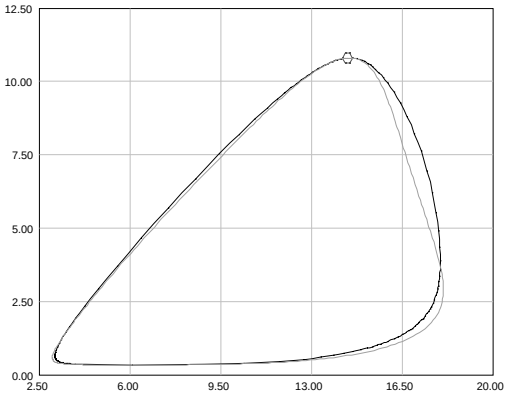

(a) Environmental contours for *swell*, 1 year return period, constructed using the Rosenblatt transformation (grey curve) and using Monte Carlo simulation (black curve). The small marker defines the starting point of the Rosenblatt contour.

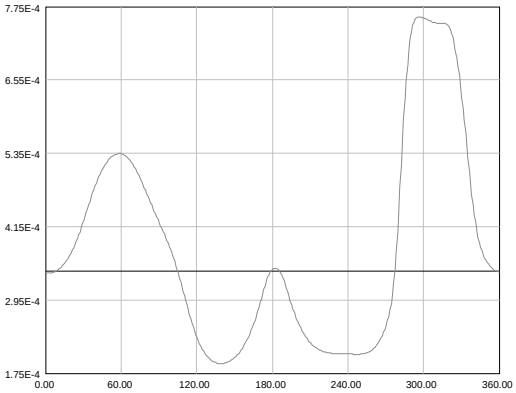

(b) $P[(T,H) \in \tilde{\mathcal{F}}(x)]$ as a function of the point $x \in \partial\mathcal{B}$ for *swell*, 1 year return period, for the Rosenblatt contour (grey curve). The black curve represents the desired exceedence probability $P_e = 3.4223 \cdot 10^{-4}$.

Figure 19: West Shetland, swell, 1 year return period.

3.1.2 *West of Africa*

Table 3: Fitted parameter for the three-parameter Weibull distribution for signifcant wave heights.

	α	β	γ
Swell	0.709	1.688	0.297

Table 4: Fitted parameter for the conditional log-normal distribution for wave periods.

		$i=1$	$i=2$	$i=3$
Swell	a_i	0.100	2.146	0.193
	b_i	0.035	0.957	-1.053

Swell

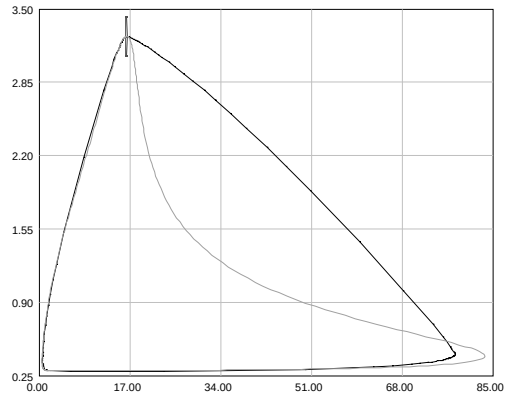

(a) Environmental contours for *swell*, 25 years return period, constructed using the Rosenblatt transformation (grey curve) and using Monte Carlo simulation (black curve). The small marker defines the starting point of the Rosenblatt contour.

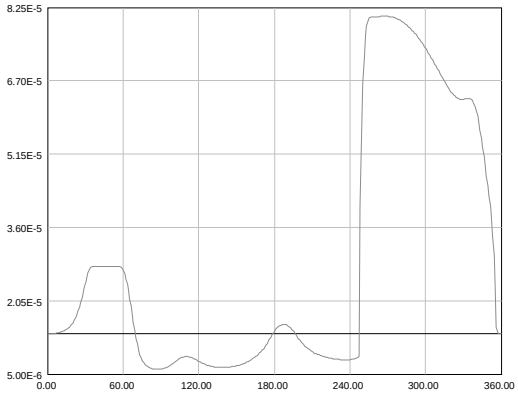

(b) $P[(T,H) \in \tilde{\mathcal{F}}(x)]$ as a function of the point $x \in \partial\mathcal{B}$ for *swell*, 25 years return period, for the Rosenblatt contour (grey curve). The black curve represents the desired exceedence probability $P_e = 1.3689 \cdot 10^{-5}$.

Figure 20: West of Africa, swell, 25 years return period.

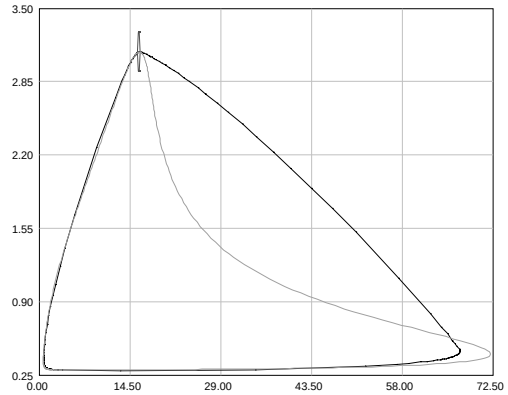

(a) Environmental contours for *swell*, 10 years return period, constructed using the Rosenblatt transformation (grey curve) and using Monte Carlo simulation (black curve). The small marker defines the starting point of the Rosenblatt contour.

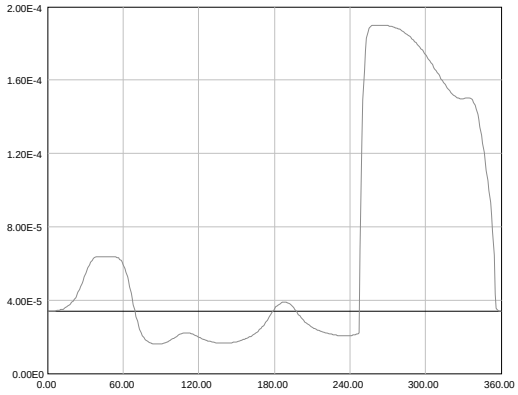

(b) $P[(T,H) \in \tilde{\mathcal{F}}(x)]$ as a function of the point $x \in \partial\mathcal{B}$ for *swell*, 10 years return period, for the Rosenblatt contour (grey curve). The black curve represents the desired exceedence probability $P_e = 3.4223 \cdot 10^{-5}$.

Figure 21: West of Africa, swell, 10 years return period.

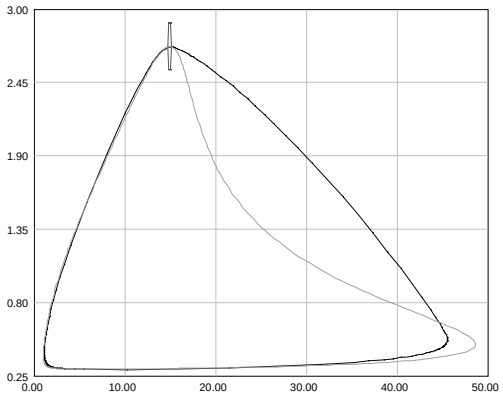

(a) Environmental contours for *swell*, 1 year return period, constructed using the Rosenblatt transformation (grey curve) and using Monte Carlo simulation (black curve). The small marker defines the starting point of the Rosenblatt contour.

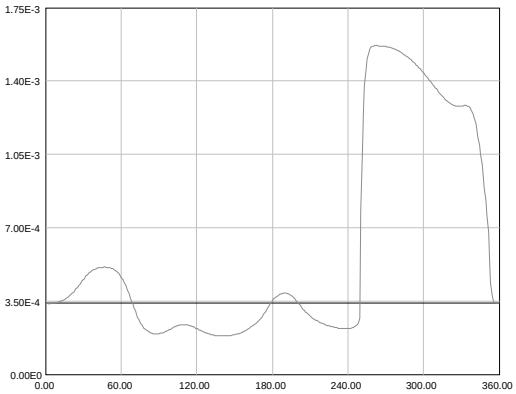

(b) $P[(T,H) \in \tilde{\mathcal{F}}(x)]$ as a function of the point $x \in \partial\mathcal{B}$ for *swell*, 1 year return period, for the Rosenblatt contour (grey curve). The black curve represents the desired exceedence probability $P_e = 3.4223 \cdot 10^{-4}$.

Figure 22: West of Africa, swell, 1 year return period.

3.1.3 *Northwest of Australia*

Table 5: Fitted parameter for the three-parameter Weibull distribution for signifcant wave heights.

	α	β	γ
Total sea	0.606	0.892	0.452
Wind sea	0.605	0.867	0.322
Swell	0.450	1.580	0.132

Table 6: Fitted parameter for the conditional log-normal distribution for wave periods.

		$i=1$	$i=2$	$i=3$
Total sea	a_i	0.750	1.150	0.153
	b_i	0.061	0.882	-1.023
Wind sea	a_i	0.000	1.798	0.134
	b_i	0.042	0.224	-0.500
Swell	a_i	0.010	2.543	0.032
	b_i	0.137	0.000	0.000

Total sea

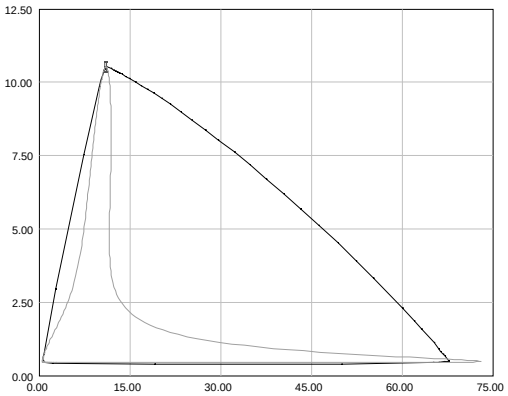

(a) Environmental contours for *total sea*, 25 years return period, constructed using the Rosenblatt transformation (grey curve) and using Monte Carlo simulation (black curve). The small marker defines the starting point of the Rosenblatt contour.

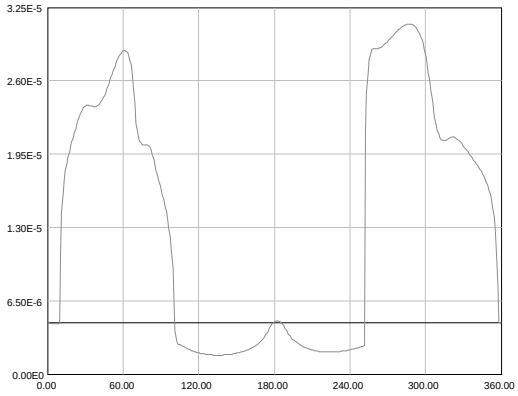

(b) $P[(T,H) \in \tilde{\mathcal{F}}(x)]$ as a function of the point $x \in \partial\mathcal{B}$ for *total sea*, 25 years return period, for the Rosenblatt contour (grey curve). The black curve represents the desired exceedence probability $P_e = 4.5631 \cdot 10^{-6}$.

Figure 23: Northwest of Australia, total sea, 25 years return period.

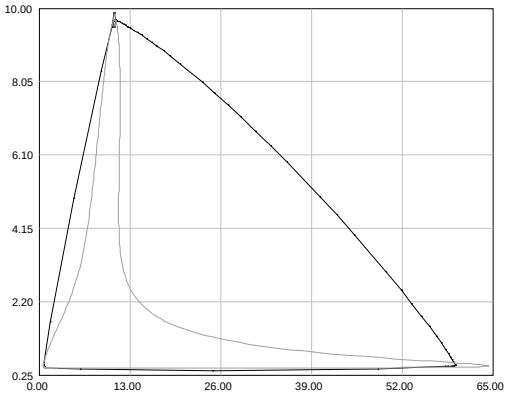

(a) Environmental contours for *total sea*, 10 years return period, constructed using the Rosenblatt transformation (grey curve) and using Monte Carlo simulation (black curve). The small marker defines the starting point of the Rosenblatt contour.

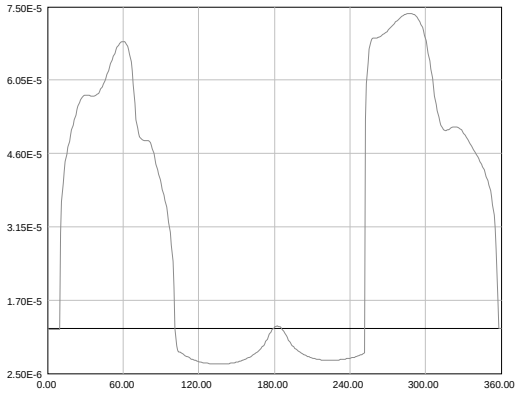

(b) $P[(T,H) \in \tilde{\mathcal{F}}(x)]$ as a function of the point $x \in \partial\mathcal{B}$ for *total sea*, 10 years return period, for the Rosenblatt contour (grey curve). The black curve represents the desired exceedence probability $P_e = 1.1408 \cdot 10^{-5}$.

Figure 24: Northwest of Australia, total sea, 10 years return period.

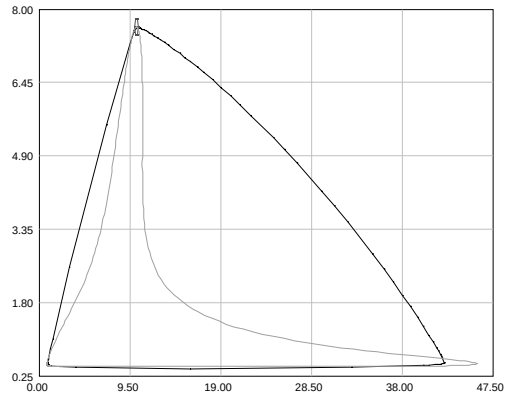

(a) Environmental contours for *total sea*, 1 year return period, constructed using the Rosenblatt transformation (grey curve) and using Monte Carlo simulation (black curve). The small marker defines the starting point of the Rosenblatt contour.

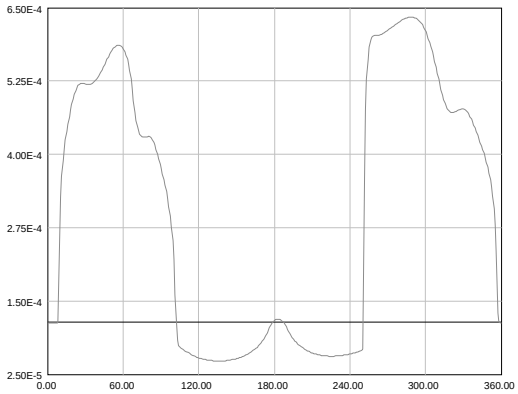

(b) $P[(T,H) \in \tilde{\mathcal{F}}(x)]$ as a function of the point $x \in \partial\mathcal{B}$ for *total sea*, 1 year return period, for the Rosenblatt contour (grey curve). The black curve represents the desired exceedence probability $P_e = 1.1408 \cdot 10^{-4}$.

Figure 25: Northwest of Australia, total sea, 1 year return period.

Wind sea

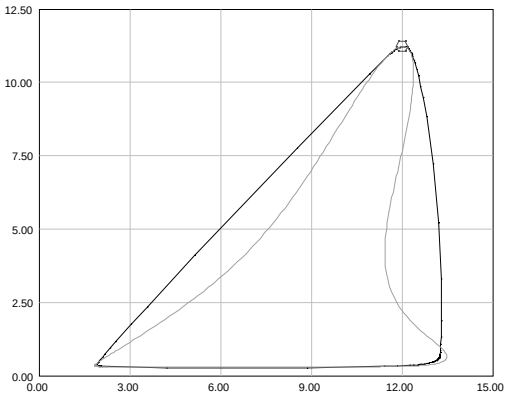

(a) Environmental contours for *wind sea*, 25 years return period, constructed using the Rosenblatt transformation (grey curve) and using Monte Carlo simulation (black curve). The small marker defines the starting point of the Rosenblatt contour.

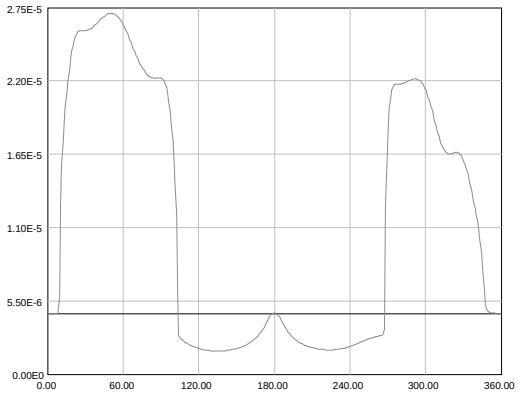

(b) $P[(T,H) \in \tilde{\mathcal{F}}(x)]$ as a function of the point $x \in \partial\mathcal{B}$ for *wind sea*, 25 years return period, for the Rosenblatt contour (grey curve). The black curve represents the desired exceedence probability $P_e = 4.5631 \cdot 10^{-6}$.

Figure 26: Northwest of Australia, wind sea, 25 years return period.

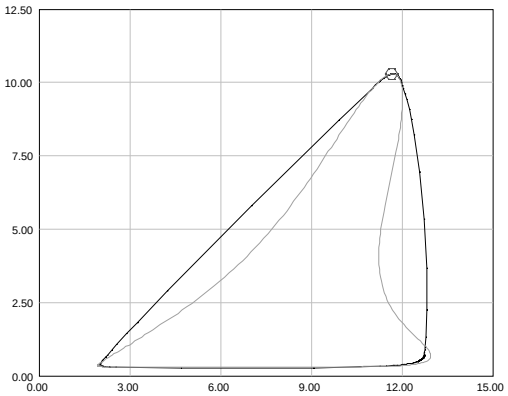

(a) Environmental contours for *wind sea*, 10 years return period, constructed using the Rosenblatt transformation (grey curve) and using Monte Carlo simulation (black curve). The small marker defines the starting point of the Rosenblatt contour.

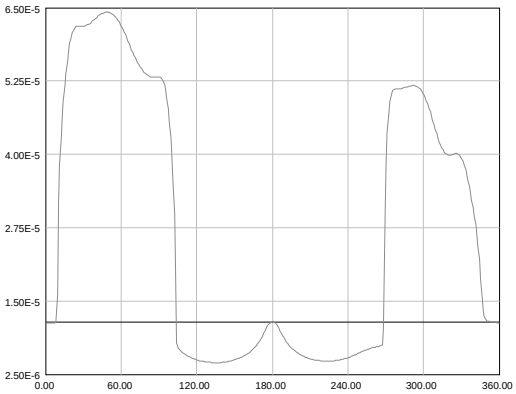

(b) $P[(T,H) \in \tilde{\mathcal{F}}(x)]$ as a function of the point $x \in \partial\mathcal{B}$ for *wind sea*, 10 years return period, for the Rosenblatt contour (grey curve). The black curve represents the desired exceedence probability $P_e = 1.1408 \cdot 10^{-5}$.

Figure 27: Northwest of Australia, wind sea, 10 years return period.

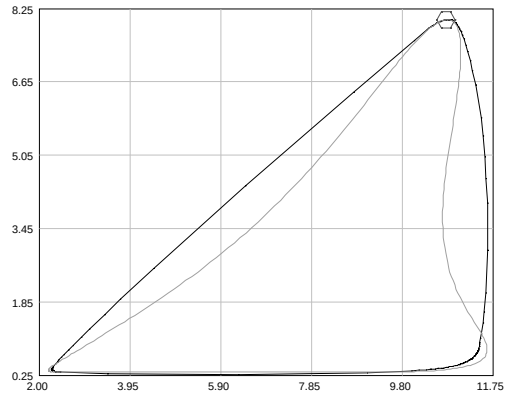

(a) Environmental contours for *wind sea*, 1 year return period, constructed using the Rosenblatt transformation (grey curve) and using Monte Carlo simulation (black curve). The small marker defines the starting point of the Rosenblatt contour.

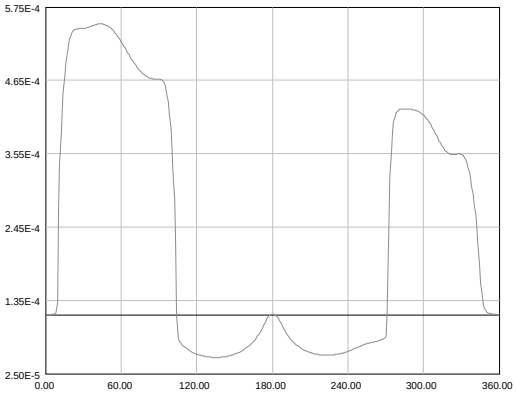

(b) $P[(T,H) \in \tilde{\mathcal{F}}(x)]$ as a function of the point $x \in \partial\mathcal{B}$ for *wind sea*, 1 year return period, for the Rosenblatt contour (grey curve). The black curve represents the desired exceedence probability $P_e = 1.1408 \cdot 10^{-4}$.

Figure 28: Northwest of Australia, wind sea, 1 year return period.

Swell

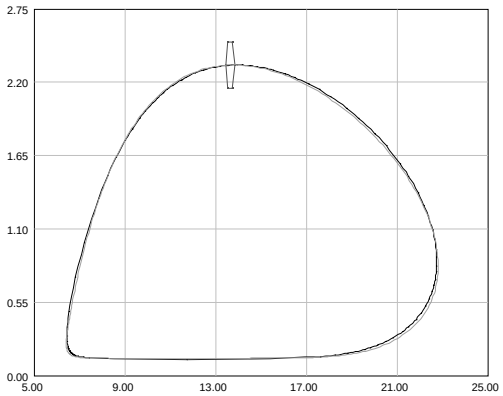

(a) Environmental contours for *swell*, 25 years return period, constructed using the Rosenblatt transformation (grey curve) and using Monte Carlo simulation (black curve). The small marker defines the starting point of the Rosenblatt contour.

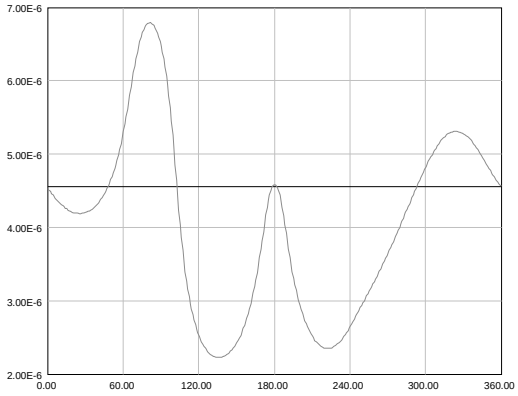

(b) $P[(T,H) \in \tilde{\mathcal{F}}(x)]$ as a function of the point $x \in \partial\mathcal{B}$ for *swell*, 25 years return period, for the Rosenblatt contour (grey curve). The black curve represents the desired exceedence probability $P_e = 4.5631 \cdot 10^{-6}$.

Figure 29: Northwest of Australia, swell, 25 years return period.

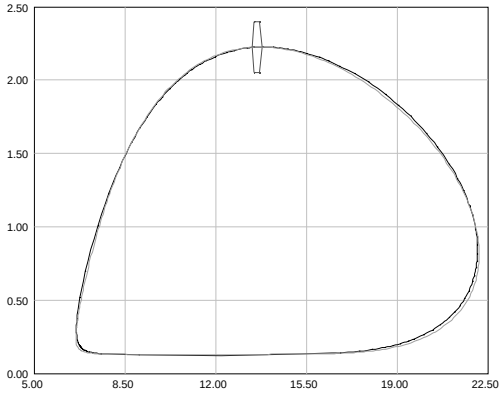

(a) Environmental contours for *swell*, 10 years return period, constructed using the Rosenblatt transformation (grey curve) and using Monte Carlo simulation (black curve). The small marker defines the starting point of the Rosenblatt contour.

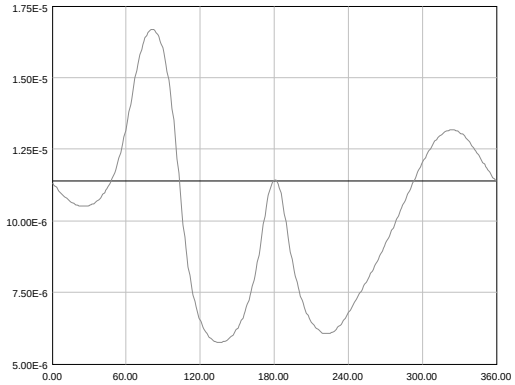

(b) $P[(T,H) \in \tilde{\mathcal{F}}(x)]$ as a function of the point $x \in \partial\mathcal{B}$ for *swell*, 10 years return period, for the Rosenblatt contour (grey curve). The black curve represents the desired exceedence probability $P_e = 1.1408 \cdot 10^{-5}$.

Figure 30: Northwest of Australia, swell, 10 years return period.

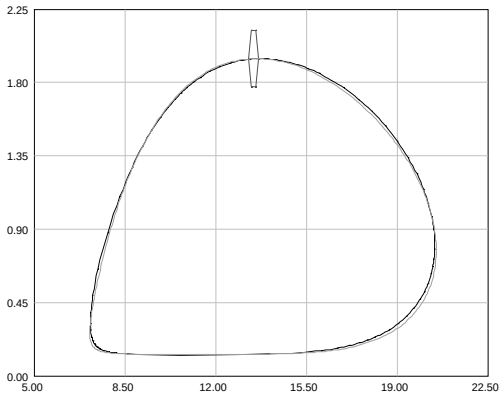

(a) Environmental contours for *swell*, 1 year return period, constructed using the Rosenblatt transformation (grey curve) and using Monte Carlo simulation (black curve). The small marker defines the starting point of the Rosenblatt contour.

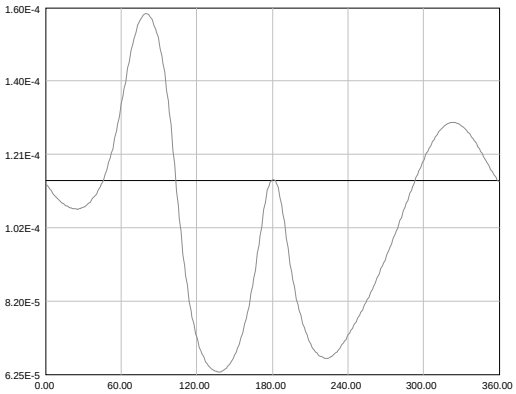

(b) $P[(T,H) \in \tilde{\mathcal{F}}(x)]$ as a function of the point $x \in \partial\mathcal{B}$ for *swell*, 1 year return period, for the Rosenblatt contour (grey curve). The black curve represents the desired exceedence probability $P_e = 1.1408 \cdot 10^{-4}$.

Figure 31: Northwest of Australia, swell, 1 year return period.

West Shetland

Type of sea	**Return period**	**Desired exceedance probability**	**Upper bound on the exceedance probability**	**x-coordinates**
Total sea	25 years	$1.3689 \cdot 10^{-5}$	$5.1445 \cdot 10^{-5}$	$(20.42, 4.37)$
	10 years	$3.4223 \cdot 10^{-5}$	$1.1765 \cdot 10^{-4}$	$(19.60, 4.57)$
	1 year	$3.4223 \cdot 10^{-4}$	$8.7393 \cdot 10^{-4}$	$(17.60, 5.14)$
Wind sea	25 years	$1.3689 \cdot 10^{-5}$	$8.6806 \cdot 10^{-5}$	$(5.77, 2.51)$
	10 years	$3.4223 \cdot 10^{-5}$	$2.0714 \cdot 10^{-4}$	$(5.80, 2.48)$
	1 year	$3.4223 \cdot 10^{-4}$	0.0018	$(5.91, 2.38)$
Swell	25 years	$1.3689 \cdot 10^{-5}$	$4.7138 \cdot 10^{-5}$	$(20.36, 4.36)$
	10 years	$3.4223 \cdot 10^{-5}$	$1.0643 \cdot 10^{-4}$	$(19.46, 4.69)$
	1 year	$3.4223 \cdot 10^{-4}$	$7.5871 \cdot 10^{-4}$	$(17.39, 5.44)$

Table 7: The largest value of $P[(T, H) \in \tilde{\mathcal{F}}(x)]$ as a function of the point $x \in \partial\mathcal{B}$, i.e., the upper bound on the exceedance probability, with the corresponding x-coordinates and the desired exceedance probabilities for every type of sea and return period for West Shetland.

West of Africa

Type of sea	**Return period**	**Desired exceedance probability**	**Upper bound on the exceedance probability**	**x-coordinates**
Swell	25 years	$1.3689 \cdot 10^{-5}$	$8.0733 \cdot 10^{-5}$	$(55.37, 0.81)$
	10 years	$3.4223 \cdot 10^{-5}$	$1.9002 \cdot 10^{-4}$	$(51.76, 0.79)$
	1 year	$3.4223 \cdot 10^{-4}$	0.0016	$(42.34, 0.72)$

Table 8: The largest value of $P[(T, H) \in \tilde{\mathcal{F}}(x)]$ as a function of the point $x \in \partial\mathcal{B}$, i.e., the upper bound on the exceedance probability, with the corresponding x-coordinates and the desired exceedance probabilities for every type of sea and return period for West of Africa.

Northwest of Australia

Type of sea	**Return period**	**Desired exceedance probability**	**Upper bound on the exceedance probability**	**x-coordinates**
Total sea	25 years	$4.5631 \cdot 10^{-6}$	$3.1074 \cdot 10^{-5}$	$(15.24, 2.12)$
	10 years	$1.1408 \cdot 10^{-5}$	$7.3812 \cdot 10^{-5}$	$(15.21, 2.03)$
	1 year	$1.1408 \cdot 10^{-4}$	$6.3456 \cdot 10^{-4}$	$(14.51, 1.89)$
Wind sea	25 years	$4.5631 \cdot 10^{-6}$	$2.7117 \cdot 10^{-5}$	$(7.59, 5.05)$
	10 years	$1.1408 \cdot 10^{-5}$	$6.4318 \cdot 10^{-5}$	$(7.68, 5.01)$
	1 year	$1.1408 \cdot 10^{-4}$	$5.5009 \cdot 10^{-4}$	$(7.74, 4.66)$
Swell	25 years	$4.5631 \cdot 10^{-6}$	$6.7988 \cdot 10^{-6}$	$(6.81, 0.67)$
	10 years	$1.1408 \cdot 10^{-5}$	$1.6705 \cdot 10^{-5}$	$(6.99, 0.66)$
	1 year	$1.1408 \cdot 10^{-4}$	$1.5845 \cdot 10^{-4}$	$(7.57, 0.67)$

Table 9: The largest value of $P[(T, H) \in \tilde{\mathcal{F}}(x)]$ as a function of the point $x \in \partial\mathcal{B}$, i.e., the upper bound on the exceedance probability, with the corresponding x-coordinates and the desired exceedance probability for every type of sea and return period for Northwest of Australia.

Summarizing all the results from these examples we see that the upper bound on the exceedance probability is larger than the desired exceedance probability for all cases. From the plots of the upper bound on the exceedance probability, we observe that there are points where the curve is below the desired value as well. However, the average value of the curve is obviously greater than the desired exceedence probability, except for the Northwest of Australia, swell case. Typically, the points where curve is above the desired value corresponds to points on the Rosenblatt contour which are inside the Monte Carlo contour, while the points where curve is below the desired value corresponds to points on the Rosenblatt contour which are outside the Monte Carlo contour.

We also observe that the value of $P[(T, H) \in \tilde{\mathcal{F}}(x)]$ varies a lot as the point x is moved along the contours. This indicates that design based on these contours may not have the desired failure probability. In fact, depending on the chosen design point, the failure probability may be considerably greater than the desired value, but it may also be lower than this value. In contrast environmental contours obtained using the Monte Carlo simulation approach will always have the desired exceedence probability. Thus, in cases

where the true failure region is convex, design based on these contours will have a failure probability which is less than or equal to the desired exceedence probability.

While the results for the environmental contours obtained using the Rosenblatt transformation are unsatisfactory, we should keep in mind that since most of these contours, except for Northwest of Australia, swell case, are clearly not convex, the upper bound can be crude. In the next section we shall investigate this further.

4 LOCALLY CONCAVE SEGMENTS

We recall from the examples considered in the previous section, that the probability $P[(T,H) \in \tilde{\mathcal{F}}(x)]$ typically had its highest values whenever the point x was located in a part of the contour which was strongly non-convex. In this section we would like to derive a method for identifying a maximal convex failure region which covers such a part. In order to do so, we parametrize the contour ∂B. That is, we assume that we have found functions g_t og g_h and an interval $\Omega \subseteq \mathbb{R}$ such that:

$$\partial\mathcal{B} = \{(t,h) = (g_t(s), g_h(s)) : s \in \Omega\}.$$

Intuitively, this means that when the parameter s runs through the interval Ω, then the point $(g_t(s), g_h(s))$ runs through $\partial\mathcal{B}$. As a convention we always choose the parametrization so that each of the points in $\partial\mathcal{B}$ occurs exactly once as s runs through Ω, and such that the point $(g_t(s), g_h(s))$ runs through $\partial\mathcal{B}$ counterclockwise as s runs through Ω from the lowest to the highest value.

We now define the concepts of *local convexity* and *local concavity* for the contour $\partial\mathcal{B}$ as follows. We say that $\partial\mathcal{B}$ is *locally convex* at the point $(t,h) = (g_t(s), g_h(s))$, where $s \in \Omega$, if there exists an open interval $\Omega_s \subseteq \Omega$ where $s \in \Omega_s$, such that for all $s_1, s_2 \in \Omega_s$ the line segment between the points $(g_t(s_1), g_h(s_1))$ and $(g_t(s_2), g_h(s_2))$ is entirely contained in $\mathcal{B}$. Similarly, we say that $\partial\mathcal{B}$ is *locally concave* in the point $(t,h) = (g_t(s), g_h(s))$, where $s \in \Omega$, if there exists an open interval $\Omega_s \subseteq \Omega$ where $s \in \Omega_s$, such that for all $s_1, s_2 \in \Omega_s$ the line segment between the points $(g_t(s_1), g_h(s_1))$ and $(g_t(s_2), g_h(s_2))$ is entirely (except for the end points) contained in the complement of $\mathcal{B}$. Note that if $\mathcal{B}$ is locally convex at a point (t,h), then the complement of $\mathcal{B}$ is locally concave at the same point. Similarly, if $\mathcal{B}$ is locally concave at a point (t,h), then the complement of $\mathcal{B}$ is locally convex at the same point.

To find intervals where $\mathcal{B}$ is locally concave, we move along $\partial\mathcal{B}$ counterclockwise and identify whether angles between line segments are positive or negative as explained in Figure 4. We notice that if we get an positive angle between the line segments we get a *left turn* which corresponds to local convexity, while if the angle between line segments is negative, we get a *right turn* which corresponds to local concavity. By using this interpretation it is possible to construct an algorithm for identifying intervals of points where $\partial\mathcal{B}$ is locally concave. See Figure 32.

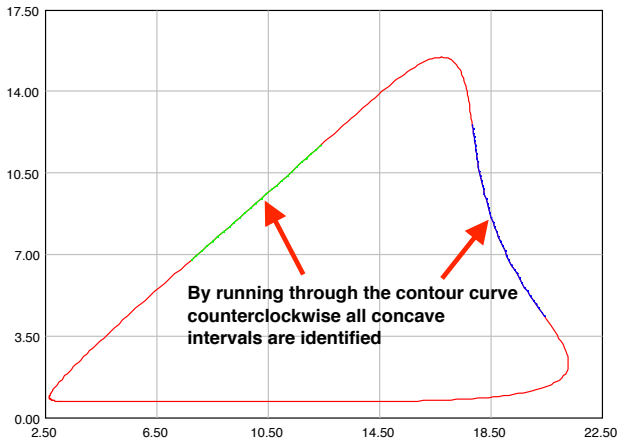

Figure 32: Identifying intervals of points where $\partial\mathcal{B}$ is locally concave.

Having identified these locally concave intervals we use the fact that the complement of $\mathcal{B}$ is locally convex in the same intervals. Thus, we can construct maximal convex failure regions by extending these intervals of $\partial\mathcal{B}$ by straight lines, and let these maximal failure regions be the area separated from $\mathcal{B}$ by the resulting lines. See Figure 33. Since $\mathcal{B}$ typically has a smooth boundary, there will only be a finite number of such maximal convex failure regions. It is then easy to estimate the failure probabilities associated with these maximal failure regions using Monte Carlo simulation. The exceedence probability can then be estimated by taking the maximum of these estimated probabilities.

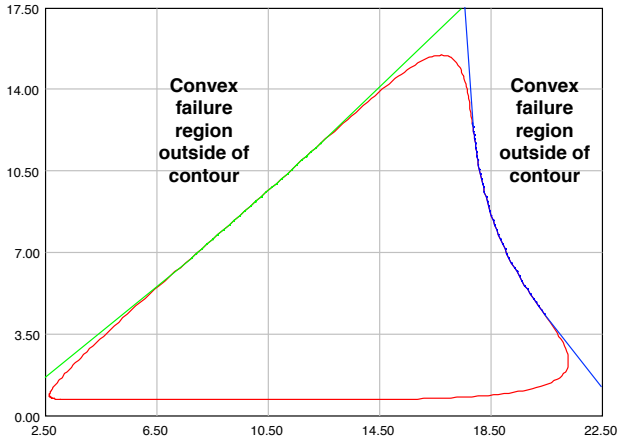

Figure 33: Maximal convex failure regions outside of contour.

4.1 *Numerical examples*

In this subsection we proceed with all the examples introduced in Subsection 3.1, and compute the exceedence probability by identifying the intervals of points where $\partial\mathcal{B}$ is locally concave. We then construct maximal convex failure regions by extending these parts of $\partial\mathcal{B}$ by straight lines as shown in Figure 33. The resulting estimated exceedence probabilities, $P_e(\mathcal{B}, \mathcal{E})$, for every type of sea are listed in the following tables for every lo-

cation and every return period. In the tables we have also included the desired exceedance probabilites and the upper bound on the exceedance probabiliy from Subsection 3.1.

4.1.1 *West Shetland*

25 years return period

Type of sea	$P_e(\mathcal{B}, \mathcal{E})$	**Desired exceedance probability**	**Upper bound on the exceedance probability**
Total sea	$3.7327 \cdot 10^{-5}$	$1.3689 \cdot 10^{-5}$	$5.1445 \cdot 10^{-5}$
Wind sea	$3.8988 \cdot 10^{-5}$	$1.3689 \cdot 10^{-5}$	$8.6806 \cdot 10^{-5}$
Swell	$3.6190 \cdot 10^{-5}$	$1.3689 \cdot 10^{-5}$	$4.7138 \cdot 10^{-5}$

Table 10: West Shetland, 25 years return period.

10 years return period

Type of sea	$P_e(\mathcal{B}, \mathcal{E})$	**Desired exceedance probability**	**Upper bound on the exceedance probability**
Total sea	$8.9620 \cdot 10^{-5}$	$3.4223 \cdot 10^{-5}$	$1.1765 \cdot 10^{-4}$
Wind sea	$9.6825 \cdot 10^{-5}$	$3.4223 \cdot 10^{-5}$	$2.0714 \cdot 10^{-4}$
Swell	$8.7421 \cdot 10^{-5}$	$3.4223 \cdot 10^{-5}$	$1.0643 \cdot 10^{-4}$

Table 11: West Shetland, 10 years return period.

1 year return period

Type of sea	$P_e(\mathcal{B}, \mathcal{E})$	**Desired exceedance probability**	**Upper bound on the exceedance probability**
Total sea	$7.7166 \cdot 10^{-4}$	$3.4223 \cdot 10^{-4}$	$8.7393 \cdot 10^{-4}$
Wind sea	$9.1372 \cdot 10^{-4}$	$3.4223 \cdot 10^{-4}$	0.0018
Swell	$7.3533 \cdot 10^{-4}$	$3.4223 \cdot 10^{-4}$	$7.5871 \cdot 10^{-4}$

Table 12: West Shetland, 1 year return period.

4.1.2 *West of Africa*

25 years return period

Type of sea	$P_e(\mathcal{B}, \mathcal{E})$	**Desired exceedance probability**	**Upper bound on the exceedance probability**
Swell	$4.6939 \cdot 10^{-5}$	$1.3689 \cdot 10^{-5}$	$8.0733 \cdot 10^{-5}$

Table 13: West of Africa, 25 years return period

10 years return period

Type of sea	$P_e(\mathcal{B}, \mathcal{E})$	**Desired exceedance probability**	**Upper bound on the exceedance probability**
Swell	$1.1483 \cdot 10^{-4}$	$3.4223 \cdot 10^{-5}$	$1.9002 \cdot 10^{-4}$

Table 14: West of Africa, 10 years return period.

1 year return period

Type of sea	$P_e(\mathcal{B}, \mathcal{E})$	**Desired exceedance probability**	**Upper bound on the exceedance probability**
Swell	0.0010	$3.4223 \cdot 10^{-4}$	0.0016

Table 15: West of Africa, 1 year return period.

4.1.3 *Northwest of Australia*

25 years return period

Type of sea	$P_e(\mathcal{B}, \mathcal{E})$	**Desired exceedance probability**	**Upper bound on the exceedance probability**
Total sea	$1.2558 \cdot 10^{-5}$	$4.5631 \cdot 10^{-6}$	$3.1074 \cdot 10^{-5}$
Wind sea	$1.4549 \cdot 10^{-5}$	$4.5631 \cdot 10^{-6}$	$2.7117 \cdot 10^{-5}$
Swell	-	$4.5631 \cdot 10^{-6}$	$6.7988 \cdot 10^{-6}$

Table 16: Northwest of Australia, 25 years return period.

10 years return period

Type of sea	$P_e(\mathcal{B}, \mathcal{E})$	**Desired exceedance probability**	**Upper bound on the exceedance probability**
Total sea	$3.1283 \cdot 10^{-5}$	$1.1408 \cdot 10^{-5}$	$7.3812 \cdot 10^{-5}$
Wind sea	$3.6386 \cdot 10^{-5}$	$1.1408 \cdot 10^{-5}$	$6.4318 \cdot 10^{-5}$
Swell	-	$1.1408 \cdot 10^{-5}$	$1.6705 \cdot 10^{-5}$

Table 17: Northwest of Australia, 10 years return period.

1 year return period

Type of sea	$P_e(\mathcal{B}, \mathcal{E})$	**Desired exceedance probability**	**Upper bound on the exceedance probability**
Total sea	$3.1261 \cdot 10^{-4}$	$1.1408 \cdot 10^{-4}$	$6.3456 \cdot 10^{-4}$
Wind sea	$3.3596 \cdot 10^{-4}$	$1.1408 \cdot 10^{-4}$	$5.009 \cdot 10^{-4}$
Swell	-	$1.1408 \cdot 10^{-4}$	$1.5845 \cdot 10^{-4}$

Table 18: Northwest of Australia, 1 year return period.

For Northwest of Australia, in the swell case for all return periods, the contour has no such locally concave intervals. For the other cases, we observe that these probabilities are smaller than the crude upper bounds obtained by considering the maximum of $P[(T, H) \in \tilde{\mathcal{F}}(x)]$. Still for all the cases where there exists locally concave intervals, the estimated exceedence probabilities are some higher than the desired value. Thus, while the environmental contours obtained using the Rosenblatt transformation typically fits the joint distribution of the environmental variable better than the contours obtained using the Monte Carlo simulation approach, the resulting exceedance probability, as defined in this paper, may be considerably larger than desired. However, in the next section, we will adjust contours such that the exceedance probabilities becomes equal to the desired exceedance probabilities.

5 THE INVERSE PROBLEM

The inverse problem is about adjusting contours so that they obtain the same desired exceedance probability. This makes it possible to obtain contours that fit the main parts of the joint distribution better while keeping the exceedance probability under control. By adjusting the contours so that they all have the same desired exceedance probability, we can compare them directly, and find the best contour for the given application. For comparison, we now include the Iso contours.

As the Monte Carlo contours basically have the desired exceedance probability, we do not need to adjust these contours in any way. On the other hand, since the Rosenblatt contours and the Iso contours basically have exceedance probabilities higher than the desired exceedance probabilites, these need to be adjusted. Graphically, we find that the contour with the smallest area is the best. That is because we want as little requirements for the construction of the design as possible as well as we want it to be as little conservative as possible.

Before the comparison, we want to explain the techniques behind the adjustments.

5.1 *Method*

The contours are constructed by a simulation program where we specify the location, type of sea, the return period and which contour we want to obtain. In the next numerical examples we have included Iso contours in addition to the examples introduced in Subsection 3.1. We will now explain how the constructions of the contours with the desired exceedance probability is done.

The main using tool to obtain contours with the desired exceedance probability is a *P-factor*. This factor will be explained deeper in Subsection 5.2, but intuitively, an increased P-factor will expand the contours resulting in lower exceedance probability. This is especially useful for the Rosenblatt contours and the Iso contours as they basically has exceedance probability higher than desired. We always start with a P-factor=1.0 which leaves the contours unchanged. The program then uses the *bisection* method with 20 iterations in order to identify a value of P-factor which gives the contours the desired exceedance probability. The P-factor is varied within the interval $[1, 5]$. If the exceedance probability when P-factor=1.0 is too small, i.e., lower than desired, the P-factor is varied within the interval $[0.5, 5]$. For more details about the bisection method we refer to [BF85].

To see the effect of increasing the P-factor we take West Shetland, total sea, 25 years return period case as an example. For the Rosenblatt contour, the program iterates to a P-factor equal to 2.92. For the Iso contour the program iterates to a P-factor equal to 2.15. In Figure 34 we compare the Rosenblatt contours when P-factor is equal to 1.0 and P-factor equal to 2.92, and compare the Iso contours when the P-factor is equal to 1.0 and P-factor is equal to 2.15.

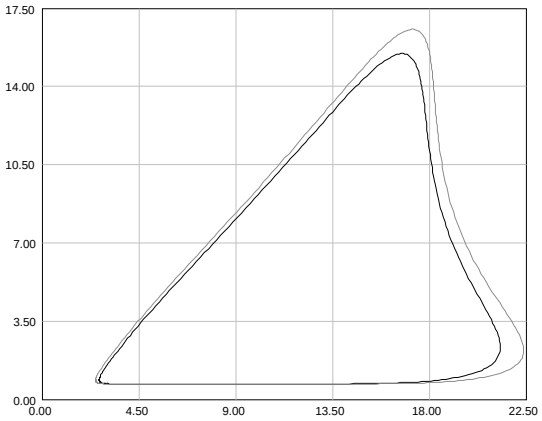

(a) Black: Rosenblatt contour, P-factor=1.0. Grey: Rosenblatt contour, P-factor=2.92

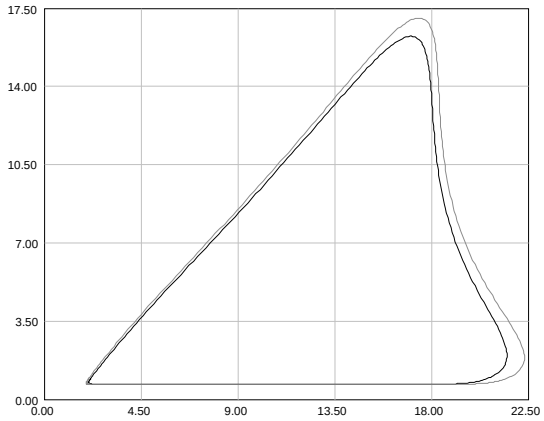

(b) Black: Iso contour, P-factor=1.0. Grey: Iso contour, P-factor=2.15

Figure 34: Effect of increasing the P-factor.

When the program has identified a P-factor giving contours with the desired exceedance probability, we will also get an adjusted return period. This is the product of the P-factor by the iterations and the original return period. For the Rosenblatt contours this adjusted return period is of interest. Continuing with the same example, West Shetland, total sea, 25 years return period, we see in Figure 35 how it looks like when we get the adjusted return period. In this case, the adjusted return period is equal to 73, i.e, $2.92 \cdot 25$ (by rounding of the P-factor to two decimals). This means that the failure we suppose will happen after 25 years must be calculated from a return period of 73 years. In Figure 35, we also see how iterations of the P-factor is working.

```
1. pfactor = 3.0, pe = 1.3327940323367993E-5
2. pfactor = 2.0, pe = 1.9688988700995276E-5
3. pfactor = 2.5, pe = 1.5879155039501435E-5
4. pfactor = 2.75, pe = 1.449953285198372E-5
5. pfactor = 2.875, pe = 1.3886105083729979E-5
6. pfactor = 2.9375, pe = 1.3605838597336125E-5
7. pfactor = 2.90625, pe = 1.3741742906552315E-5
8. pfactor = 2.921875, pe = 1.3673607345964182E-5
9. pfactor = 2.9140625, pe = 1.370861777904924E-5
10. pfactor = 2.91796875, pe = 1.3691089701953185E-5
11. pfactor = 2.919921875, pe = 1.3682342819941472E-5
12. pfactor = 2.9189453125, pe = 1.3686714833610745E-5
13. pfactor = 2.91845703125, pe = 1.3688901910800623E-5
14. pfactor = 2.918212890625, pe = 1.368999571701644E-5
15. pfactor = 2.9183349609375, pe = 1.3689448791568367E-5
16. pfactor = 2.91839599609375, pe = 1.3689175345444696E-5
17. pfactor = 2.918365478515625, pe = 1.3689312066994213E-5
18. pfactor = 2.9183807373046875, pe = 1.3689243705918744E-5
19. pfactor = 2.9183731079101562, pe = 1.3689277886458656E-5
20. pfactor = 2.918376922607422, pe = 1.3689260796034501E-5
pfactor = 2.918376922607422, pe = 1.3689260796034501E-5, exceedProb = 1.3689253935660506E-5
returnPeriod = 25.0, adjusted returnPeriod = 72.95942306518555
```

Figure 35: Adjusted return period.

It can be of interest to compare the P-factor for the Rosenblatt contours and the P-factor for the Iso contours. Since the Iso contours are constructed such that they are outside the original Rosenblatt contours as explained in Subsection 2.4, we do not, in general, need such a high P-factor value for the Iso contours as for the Rosenblatt contours.

The Monte Carlo contours do not need to be adjusted. The point is that the Monte Carlo contours are constructed such that the exceedance probabilities stabilises at the desired

exceedance probabilities at the very first time. Hence, we do not need the iterations of the P-factor as we did for the Rosenblatt contours and the Iso contours.

5.2 *P-factor - a deeper understanding*

In this subsection we will get a deeper understanding of the P-factor and what it means. We notice that a P-factor equal to, say 2.90, is not the same as saying that the exceedance probability is 2.90 times higher than the desired one. If we want to compare an exceedance probability with the desired one, we must be clear on which exceedance probability we actually mean. What is natural is to compare the exceedance probability of a contour by putting P-factor=1.0 with the desired exceedance probability.

Again, take the Rosenblatt contour for West Shetland, total sea, as an example. For a return period of 25 years, we get that the Rosenblatt contour, when P-factor =1.0, has an exceedance probability equal to $3.7888 \cdot 10^{-5}$. Since the P-factor=1.0 we can compare it to the desired exceedance probability, $1.3689 \cdot 10^{-5}$:

$$\frac{3.7888 \cdot 10^{-5}}{1.3689 \cdot 10^{-5}} = 2.77, \tag{8}$$

and hence we can say that this contour has an exceedance probability which is 2.77 times higher than the desired one.

If we iterate the P-factor such that we get a contour with the desired exceedance probability, we get a P-factor equal to 2.91. This is a number not that different from 2.77, but it is a difference. That is why it is not correct to say that the exceedance probability for that contour when P-factor=1.0 is 2.91 times higher than the desired exceedance probability.

What we in fact can say is that the Rosenblatt contour which has the desired exceedance probability and the desired return period, is evaluated from a return period which is 2.91 times as big as the return period of 25 years. That is why the program writes out an adjusted return period which is the product of 25 and 2.91. This return period corresponds to a contour with the desired exceedance probability. Alternatively we can say that the Rosenblatt contour which has the desired exceedance probability is evaluated from an exceedance probability which is equal to the desired exceedance probability divided by 2.91.

The same understanding of the P-factor applies to Iso contours as well. We start by looking at the Iso contour when P-factor=1.0. Continuing with the same example, West Shetland, total sea, with a return period equal to 25 years, we get an exceedance probability equal to $2.9141 \cdot 10^{-5}$. Again, since we have P-factor=1.0 we compare this to the desired exceedance probability, $1.3689 \cdot 10^{-5}$ and get:

$$\frac{2.9141 \cdot 10^{-5}}{1.3689 \cdot 10^{-5}} = 2.13,$$

and hence we can say that the exceedance probability we get is 2.13 times higher than the desired one. To get the Iso contour which has the desired exceedance probability, we iterate the P-factor and end up with a value of 2.16 which again is little higher than 2.13.

But why is the P-factor so close to the value which is x times higher than the desired exceedance probability? Let R_d and P_d define the desired return period and the desired exceedance probability respectively. Then the connection between R_d and P_d is as follows:

$$P_d = \frac{1}{N \cdot R_d}.$$

Where N is average number of samples per year.

Equivalently we can write:

$$R_d = \frac{1}{N \cdot P_d}.$$

As an example we choose 8 samples of data per day, as is the case for the locations West Shetland and West of Africa. Since the average number of days per year is 365.25 due to leap year every four year, we have that N is given by:

$$N = 365.25 \cdot 8.$$

Assume now that we have chosen $R_d = 25$. We then have that:

$$P_d = \frac{1}{365.25 \cdot 8 \cdot R_d} = \frac{1}{365.25 \cdot 8 \cdot 25} = \frac{1}{73050} = 1.3689 \cdot 10^{-5}.$$

Which is how we found the desired exceedance probabilities in section 3.1.

To study this further we start by constructing a Rosenblatt contour where we let P-factor=1.0 and where the desired return period $R_d = 25$ years, and the desired exceedance probability $P_d = 1.3689 \cdot 10^{-5}$. Then for West Shetland, total sea, we get a contour with two locally concave intervals with the following estimated probabilities:

$$P_1 = 3.1992 \cdot 10^{-5},$$
$$P_2 = 3.7867 \cdot 10^{-5}.$$

The exceedance probability for the Rosenblatt contour is per definition the biggest of these probabilities, i.e $P_2 = 3.7867 \cdot 10^{-5}$. We then have that:

$$\frac{P_2}{P_d} = \frac{3.7867 \cdot 10^{-5}}{1.3689 \cdot 10^{-5}} = 2.77. \tag{9}$$

We see that this is the same as in (8)[1], and again we say that P_2 is 2.77 times higher than the desired exceedance probability, P_d.

[1]Because $P_2 \approx 3.7888 \cdot 10^{-5}$. Small difference due to simulation.

More generally, let:

$P(x)$ = The exceedance probability for the Rosenblatt contour when P-factor = x,
$R(x)$ = The return period for the Rosenblatt contour when P-factor = x.

The inverse problem can then be expressed as the following equation problem:

Find x such that

$$P(x) = P_d.$$

Or alternatively and equivalently:

Find x such that

$$R(x) = R_d.$$

Based on simulations we have estimated $P(1) = P_2 = 3.7867 \cdot 10^{-5}$. We then get that:

$$R(1) = \frac{1}{N \cdot P(1)} = \frac{1}{365.25 \cdot 8 \cdot 3.7867 \cdot 10^{-5}} = 9.04.$$

And since $\frac{P(1)}{P_d} = \frac{P_2}{P_d} = 2.77$ from (9), the relation between the desired return period, R_d, and the estimated return period, $R(1)$, is naturally:

$$\frac{R_d}{R(1)} = \frac{25}{9.04} = 2.77.$$

To solve this equation with respect to $R(1)$, we then get that:

$$R(1) = \frac{R_d}{2.77}.$$

We now assume that $R(x)$ is approximately proportional to x (i.e., with the P-factor). This means that:

$$R(x) = a \cdot x,$$

for an appropariate factor a. If the assumption of the proportionality is correct, we then get that:

$$R(1) = a \cdot 1 = a.$$

At the same time we have estimated that $R(1) = 9.04 = \frac{R_d}{2.77}$. This means that the constant a is equal to $\frac{R_d}{2.77}$, and hence we get the following formula for $R(x)$:

$$R(x) = \frac{R_d}{2.77} \cdot x.$$

Given that this equation is correct we see that:

$$R(2.77) = \frac{R_d}{2.77} \cdot 2.77 = R_d.$$

Therefore it is reasonable to replace the P-factor with the value 2.77 and run simulations again hoping that this will give the desired return period and the desired exceedance probability. By doing this we got the following probabilities for the two locally concave intervals:

$$P_1 = 1.2039 \cdot 10^{-5},$$
$$P_2 = 1.4195 \cdot 10^{-5}.$$

This means that $P(2.77) = 1.4195 \cdot 10^{-5}$. Since:

$$\frac{P(2.77)}{P_d} = \frac{1.4195 \cdot 10^{-5}}{1.3689 \cdot 10^{-5}} = 1.04,$$

we have that the exceedance probability is 1.04 times higher than the desired exceedance probability. More exact we say that:

$$P(2.77) = 1.04 \cdot P_d.$$

This difference comes from that the assumption that $R(x)$ is proportional to x is not exact but still very close.

To find the x-value (i.e., the P-factor value) which gives the desired return period and the desired exceedance probability, we run iteration and find that P-factor$= x = 2.91$. This means, as already mentioned, that the exceedance probability is not 2.91 times higher than the desired one. The correct thing to say is that the Rosenblatt contour which has the desired return period and the desired exceedance probability is calculated from a return period which is 2.91 times higher than the desired return period of 25 years.

If it in contrast had been that $R(x)$ was exactly proportional to x, the correct P-factor value would actually been 2.77. At the same time it will still be that the exceedance probabilty for the original Rosenblatt contour (the one we got with a P-factor value equal to 1.0) actually is 2.77 times bigger than the desired exceedance probability. So in this case, it would have been correct saying that the relation between the exceedance probability to the original Rosenblatt contour and the desired exceedance probability was equal to the correct P-factor value.

When we evaluate the Iso contour with a P-factor=1.0 for West Shetland, total sea case, we get a contour with estimated exceedance probability $P(1) = 2.9145 \cdot 10^{-5}$. This means that:

$$\frac{P(1)}{P_d} = \frac{2.9145 \cdot 10^{-5}}{1.3689 \cdot 10^{-5}} = 2.13.$$

By changing the P-factor to 2.13 and running 5 simulations, we get the following results:

- Simulation 1: $P(2.13) = 1.3669 \cdot 10^{-5}$.
- Simulation 2: $P(2.13) = 1.3861 \cdot 10^{-5}$.

– Simulation 3: $P(2.13) = 1.3870 \cdot 10^{-5}$.

– Simulation 4: $P(2.13) = 1.3815 \cdot 10^{-5}$.

– Simulation 5: $P(2.13) = 1.4005 \cdot 10^{-5}$.

The first value is actually approximately equal to P_d, $1.3689 \cdot 10^{-5}$, but the other values are some higher which indicates that we need to increase the P-factor some. We then do 5 demands with iterations and get:

– Iteration 1: P-factor=2.168.

– Iteration 2: P-factor=2.154.

– Iteration 3: P-factor=2.150.

– Iteration 4: P-factor=2.135.

– Iteration 5: P-factor=2.170.

The average value of these is 2.16, and hence bigger than 2.13.

To summarize this we have that the Iso contour for P-factor=1.0 has an exceedance probability which is 2.13 times as big as the desired exceedance probability. The Iso contour which has the desired return period and the desired exceedance probability, is evaluated from a return period which is 2.16 times as high as the desired return period of 25 years.

5.3 *Numerical examples*

In the following examples we note that the figures will only contain the *adjusted* contours for the Rosenblatt contours and the Iso contours, and the original Monte Carlo contours. Hence, different contours for the same location and return period will have the same desired exceedance probability which makes it possible to compare the contours graphically. For every type of sea and every return period, we will first compare the adjusted Rosenblatt contour with the adjusted Iso contour, and then use the best of these to compare with the Monte Carlo contour in a different plot.

Recall the desired exceedance probabilities given in section 3.1:

For West Shetland and West of Africa, the desired exceedance probability for a return period of:

– 25 years is $1.3689 \cdot 10^{-5}$,

– 10 years is $3.4223 \cdot 10^{-5}$,

– 1 year is $3.4223 \cdot 10^{-4}$.

And for Northwest of Australia, the desired exceedance probability for a return period of:

– 25 years is $4.5631 \cdot 10^{-6}$,

– 10 years is $1.1408 \cdot 10^{-5}$,

– 1 year is $1.1408 \cdot 10^{-4}$.

We will now illustrate the inverse problem by examples considering the three locations, the three types of sea and the three different return periods as earlier in this paper.

For every location and every type of sea, we make one table for the Rosenblatt contours and one table of the Iso contours of the P-factors we got from the iterations considering all the return periods. For the Rosenblatt contours we also include the adjusted return periods in the same table. The corresponding plots are shown under the tables. We summarize the observations for every location and every type of sea after considered all the return periods.

5.3.1 *West Shetland*

Total sea

Table 19: West Shetland, total sea, Rosenblatt contours.

Return period	**P-factor from iterations**	**Adjusted return period**
25 years	2.89	$25 \cdot 2.89 \approx 72$ years
10 years	2.77	$10 \cdot 2.77 \approx 28$ years
1 year	2.43	$1 \cdot 2.42 \approx 2$ years

Table 20: West Shetland, total sea, Iso contours.

Return period	**P-factor from iterations**
25 years	2.17
10 years	2.11
1 year	1.99

From the tables we have the following corresponding figures:

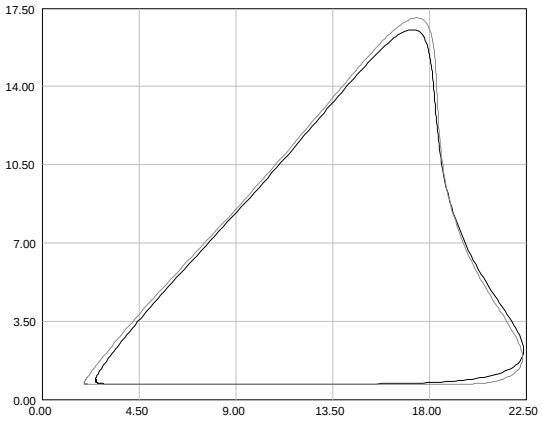

(a) Black: Rosenblatt contour, P-factor=2.89. Grey: Iso contour, P-factor=2.17.

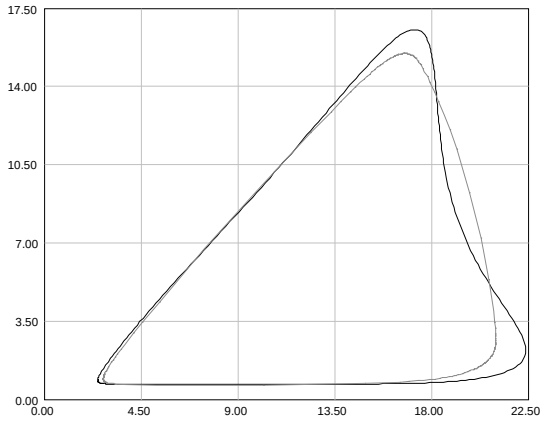

(b) Black: Rosenblatt contour, P-factor=2.89. Grey: Monte Carlo contour.

Figure 36: West Shetland, total sea, 25 years return period.

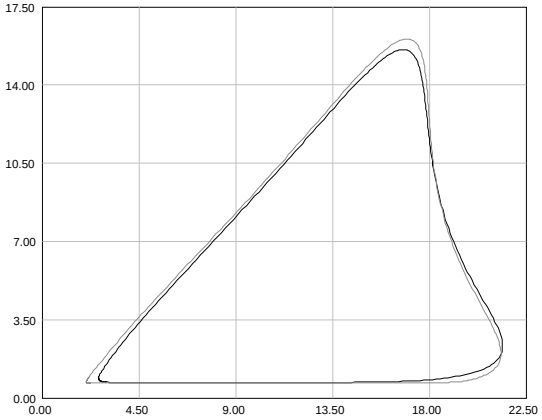

(a) Black: Rosenblatt contour, P-factor=2.77. Grey: Iso contour, P-factor=2.11.

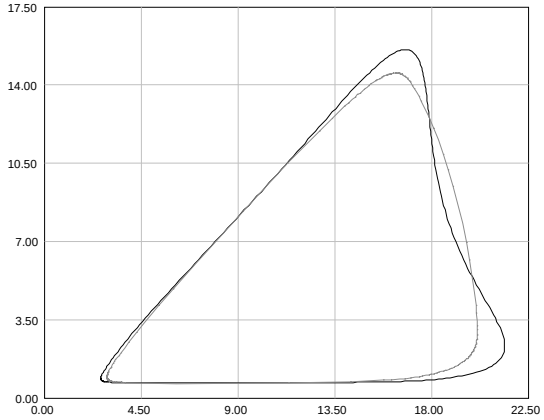

(b) Black: Rosenblatt contour, P-factor=2.77. Grey: Monte Carlo contour.

Figure 37: West Shetland, total sea, 10 years return period.

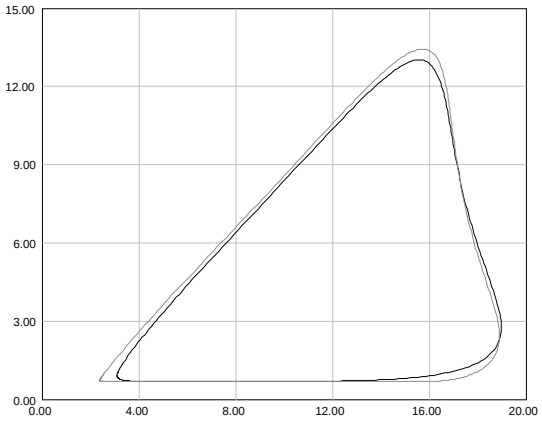

(a) Black: Rosenblatt contour, P-factor=2.43. Grey: Iso contour, P-factor=1.99.

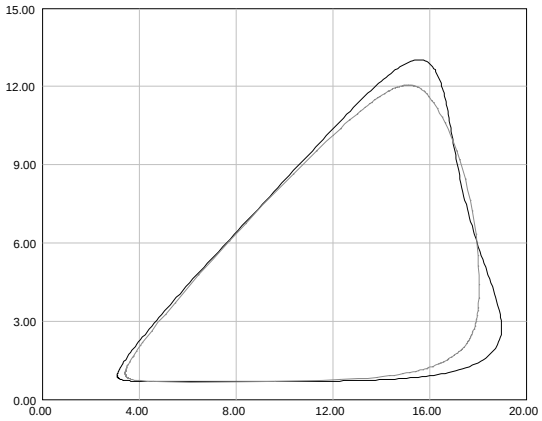

(b) Black: Rosenblatt contour, P-factor=2.43. Grey: Monte Carlo contour.

Figure 38: West Shetland, total sea, 1 year return period.

For every return period for the total sea case for West Shetland we observe that the adjusted Rosenblatt contour is the best contour compared to the adjusted Iso contour as is has the smallest area. When we then take the Monte Carlo contour into consideration, and compare this with the best adjusted contour, i.e., the adjusted Rosenblatt contour in this case, we observe that the Monte Carlo contour has the smallest area and hence is an even better contour.

Wind sea

For West Shetland, wind sea case, we have that for the Iso contours, the exceedance probabilities are too small, i.e., less than the desired exceedance probabilites. As explained in Subsection 5.1, the P-factors for these contours are varied within the interval $[0.5, 5]$.

Table 21: West Shetland, wind sea, Rosenblatt contours.

Return period	**P-factor from iterations**	**Adjusted return period**
25 years	2.90	$25 \cdot 2.90 \approx 73$ years
10 years	2.82	$10 \cdot 2.82 \approx 28$ years
1 year	2.77	$1 \cdot 2.77 \approx 3$ years

Table 22: West Shetland, wind sea, Iso contours.

Return period	**P-factor from iterations**
25 years	0.77
10 years	0.79
1 year	0.85

From the tables we have the following corresponding figures:

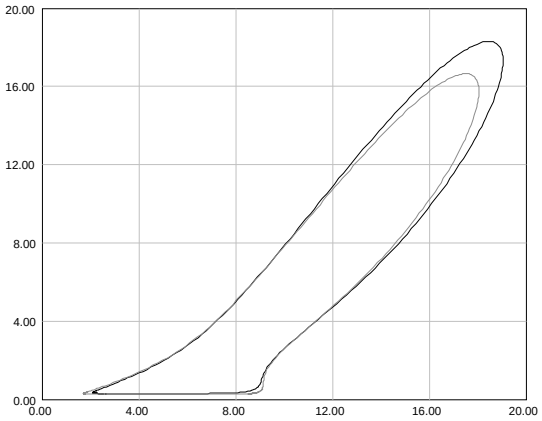

(a) Black: Rosenblatt contour, P-factor=2.90. Grey: Iso contour, P-factor=0.77.

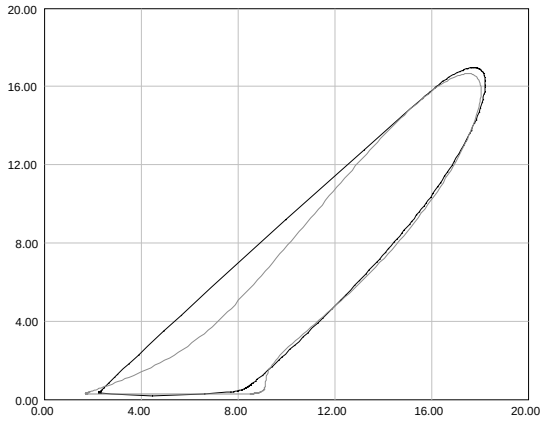

(b) Black: Monte Carlo contour. Grey: Iso contour, P-factor=0.77.

Figure 39: West Shetland, wind sea, 25 years return period.

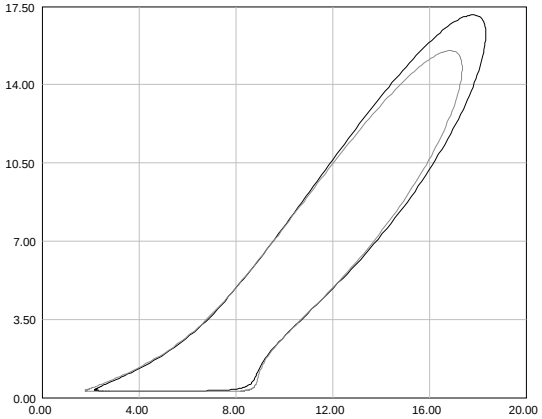

(a) Black: Rosenblatt contour, P-factor=2.82. Grey: Iso contour, P-factor=0.79.

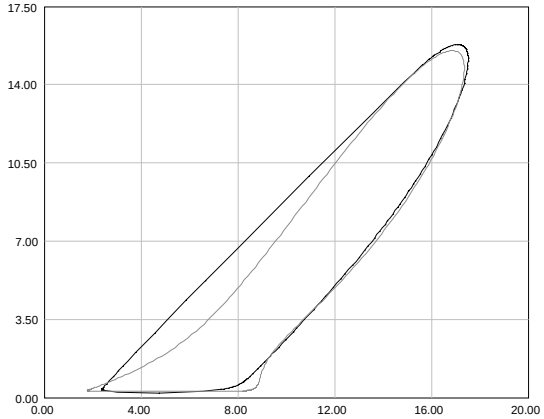

(b) Black: Monte Carlo contour. Grey: Iso contour, P-factor=0.79.

Figure 40: West Shetland, wind sea, 10 years return period.

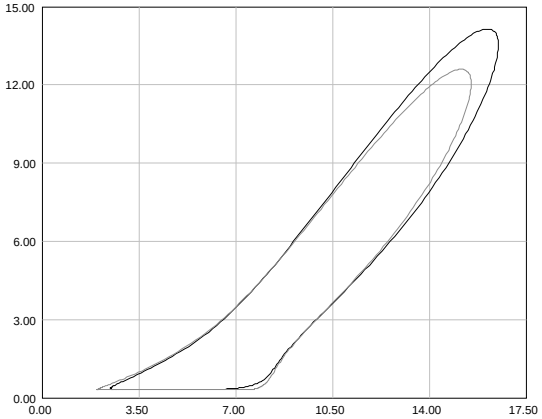

(a) Black: Rosenblatt contour, P-factor=2.77. Grey: Iso contour, P-factor=0.85.

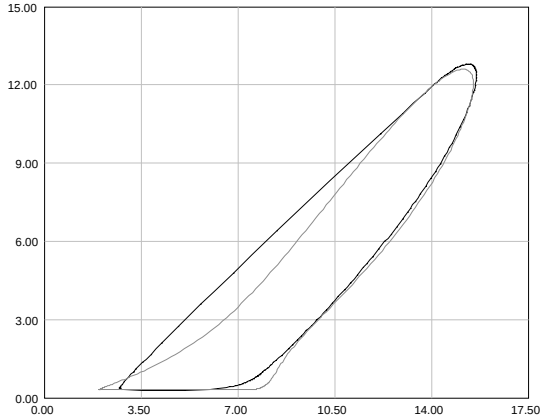

(b) Black: Monte Carlo contour. Grey: Iso contour, P-factor=0.85.

Figure 41: West Shetland, wind sea, 1 year return period.

For every return period for the wind sea case for West Shetland we observe that the adjusted Iso contour is the best contour compared to the adjusted Rosenblatt contour as it has the smallest area. When we then compare the adjusted Iso contour with the Monte Carlo contour, we observe that the adjusted Iso contour still has the smallest area, and hence is the best contour even when we take the Monte Carlo contour into consideration. Still we underline that the exceedance probability for the Iso contour is evaluated only at the locally concave regions. In this particular cases this has resulted in a contour that has slightly higher exceedance probability in the locally convex area around the topmost point. Unfortunately, this issue is not captured by our methodology.

Swell

Table 23: West Shetland, swell, Rosenblatt contours.

Return period	**P-factor from iterations**	**Adjusted return period**
25 years	2.79	$25 \cdot 2.79 \approx 70$ years
10 years	2.64	$10 \cdot 2.64 \approx 26$ years
1 year	2.30	$1 \cdot 2.30 \approx 2$ years

Table 24: West Shetland, swell, Iso contours.

Return period	**P-factor from iterations**
25 years	2.02
10 years	1.98
1 year	1.86

From the tables we have the following corresponding figures:

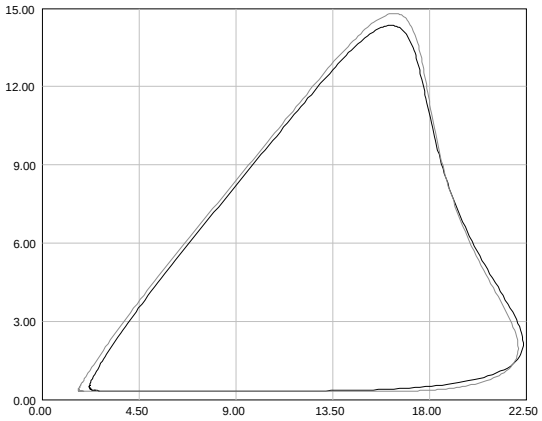

(a) Black: Rosenblatt contour, P-factor=2.79. Grey: Iso contour, P-factor=2.02.

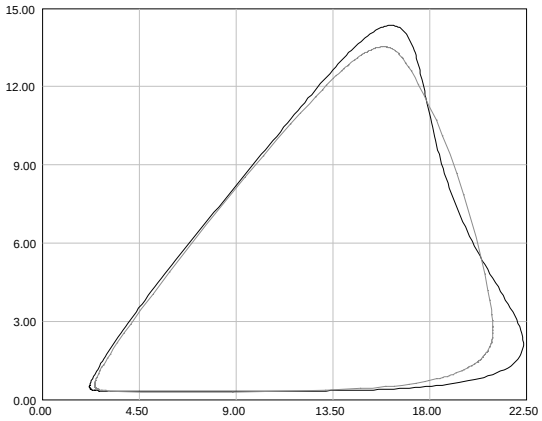

(b) Black: Rosenblatt contour, P-factor=2.79. Grey: Monte Carlo contour.

Figure 42: West Shetland, swell, 25 years return period.

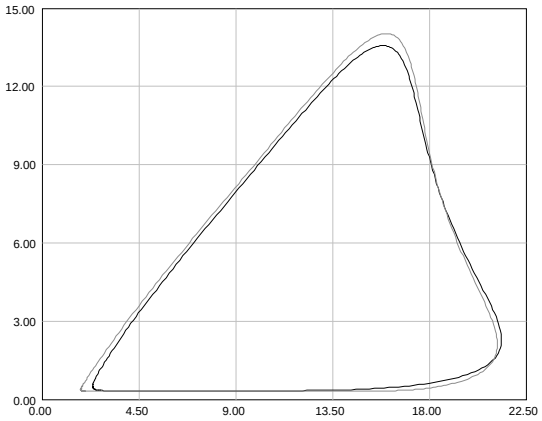

(a) Black: Rosenblatt contour, P-factor=2.64. Grey: Iso contour, P-factor=1.98.

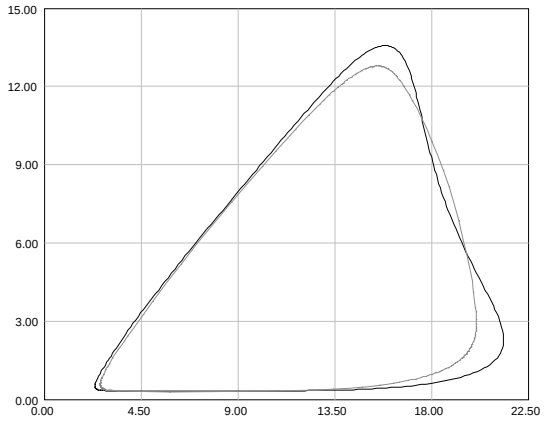

(b) Black: Rosenblatt contour, P-factor=2.64. Grey: Monte Carlo contour.

Figure 43: West Shetland, swell, 10 years return period.

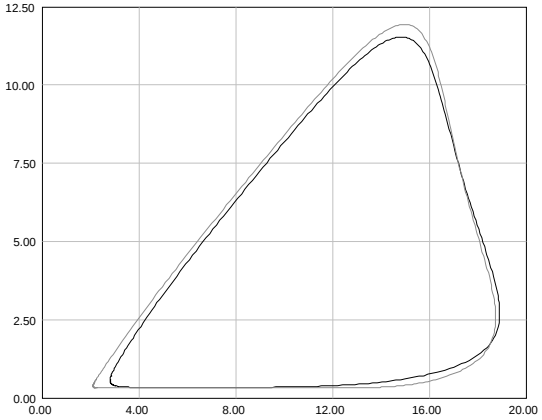

(a) Black: Rosenblatt contour, P-factor=2.30. Grey: Iso contour, P-factor=1.86.

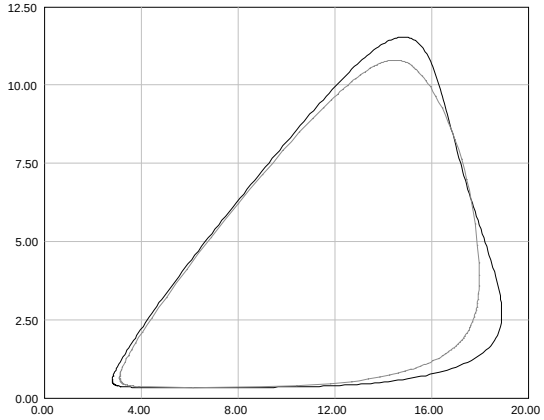

(b) Black: Rosenblatt contour, P-factor=2.30. Grey: Monte Carlo contour.

Figure 44: West Shetland, swell, 1 year return period.

For every return period for the swell case for West Shetland we observe that the adjusted Rosenblatt contour has the smallest area compared to the adjusted Iso contour, and hence is the best contour. Comparing this with the Monte Carlo contour we observe that the Monte Carlo contour has even smaller area, meaning that the Monte Carlo contour is the best contour when it is taken into consideration.

5.3.2 *West of Africa*

Swell

Table 25: West of Africa, swell, Rosenblatt contours.

Return period	**P-factor from iterations**	**Adjusted return period**
25 years	3.62	$25 \cdot 3.62 \approx 91$ years
10 years	3.50	$10 \cdot 3.50 \approx 35$ years
1 year	3.19	$1 \cdot 3.19 \approx 3$ years

Table 26: West of Africa, swell, Iso contours.

Return period	**P-factor from iterations**
25 years	1.33
10 years	1.35
1 year	1.40

From the tables we have the following corresponding figures:

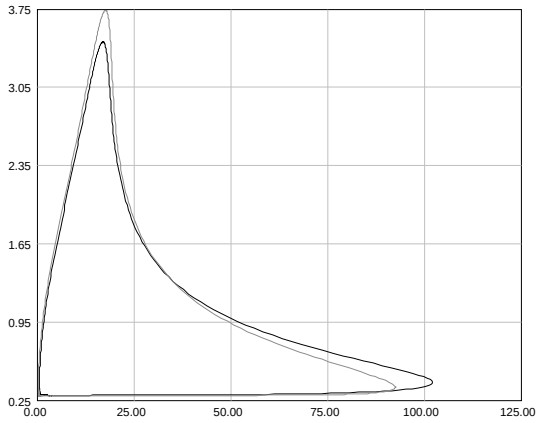

(a) Black: Rosenblatt contour, P-factor=3.62. Grey: Iso contour, 1.33.

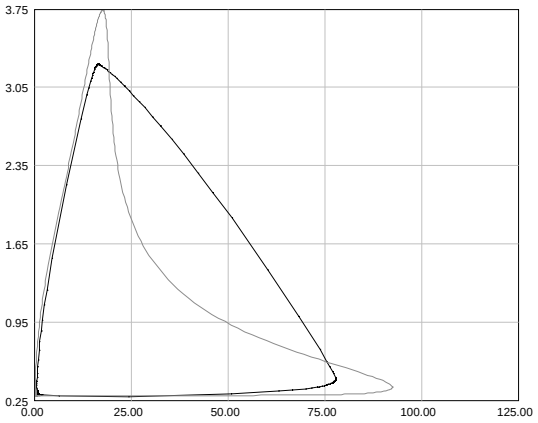

(b) Black: Monte Carlo contour. Grey: Iso contour, P-factor=1.33.

Figure 45: West of Africa, swell, 25 years return period.

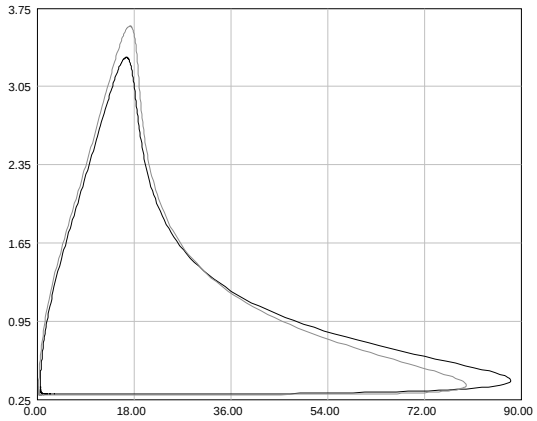

(a) Black: Rosenblatt contour, P-factor=3.50. Grey: Iso contour, P-factor=1.35.

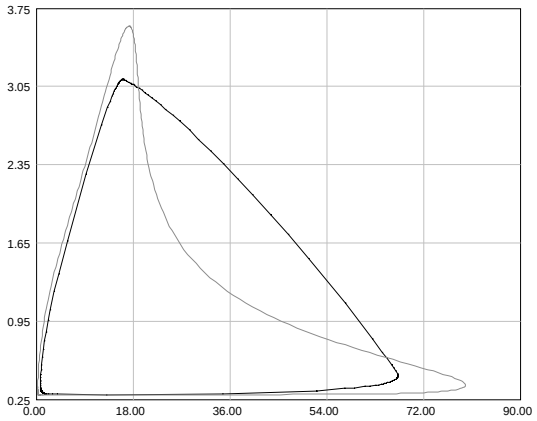

(b) Black: Monte Carlo contour. Grey: Iso contour, P-factor=1.35.

Figure 46: West of Africa, swell, 10 years return period.

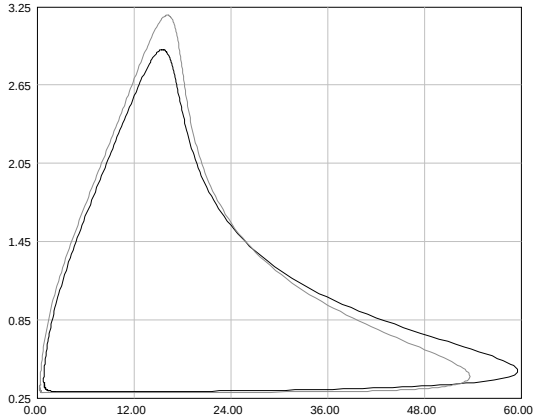

(a) Black: Rosenblatt contour, P-factor=3.19. Grey: Iso contour, P-factor=1.40.

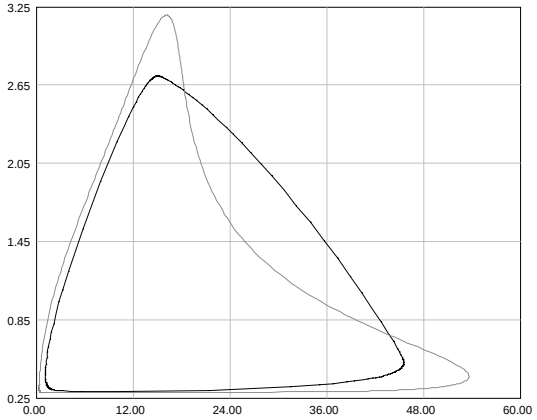

(b) Black: Monte Carlo contour. Grey: Iso contour, P-factor=1.40.

Figure 47: West of Africa, swell, 1 year return period.

Comparing the adjusted Rosenblatt contour with the adjusted Iso contour for every return period in the swell case for West of Africa, it is not that clear which contour has the smallest area. However, it might seems like the adjusted Iso contour has some smaller area than the adjusted Rosenblatt contour by looking at the lower right corner. By comparing the adjusted Iso contour with the Monte Carlo contour we observe that the adjusted Iso contour still has the smallest area. Hence, the adjusted Iso contour is the best compared to both the adjusted Rosenblatt contour and the Monte Carlo contour.

5.3.3 *Northwest of Australia*

For Northwest of Australia we recall, from Subsection 3.1, the fitted parameter for the three-parameter Weibull distribution for significant wave heights:

	α	β	γ
Total sea	0.606	0.892	0.452
Wind sea	0.605	0.867	0.322
Swell	0.450	1.580	0.132

Note that for the total sea case and wind sea case the β-values are less than 1.0. We recall from (7) that when $h \to \gamma^+$, the Iso contours, and then also the adjusted Iso contours, are not closed in these cases. Hence, the following graphs for the adjusted Iso contours will look some strange for values of h close to γ for the total sea case and wind sea case.

Total sea

Table 27: Northwest of Australia, total sea, Rosenblatt contours.

Return period	**P-factor from iterations**	**Adjusted return period**
25 years	2.77	$25 \cdot 2.77 \approx 69$ years
10 years	2.75	$10 \cdot 2.75 \approx 28$ years
1 year	2.72	$1 \cdot 2.72 \approx 3$ years

Table 28: Northwest of Australia, total sea, Iso contours.

Return period	**P-factor from iterations**
25 years	1.23
10 years	1.24
1 year	1.34

From the tables we have the following corresponding figures:

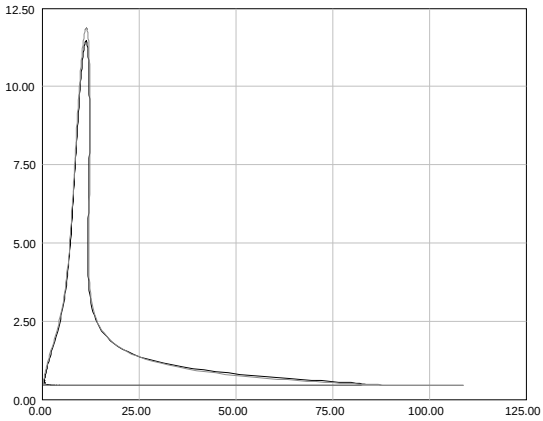

(a) Black: Rosenblatt contour, P-factor=2.77. Grey: Iso contour, P-factor=1.23.

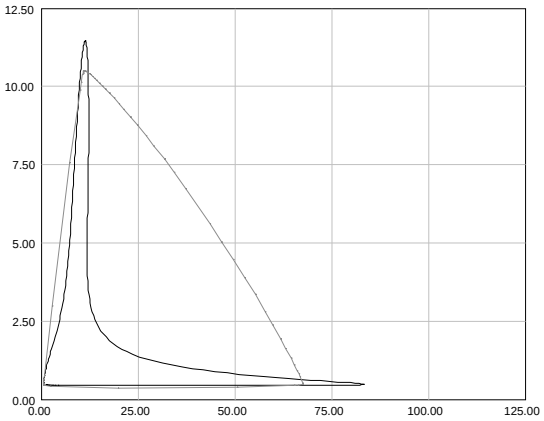

(b) Black: Rosenblatt contour, P-factor=2.77. Grey: Monte Carlo contour.

Figure 48: Northwest of Australia, total sea, 25 years return period.

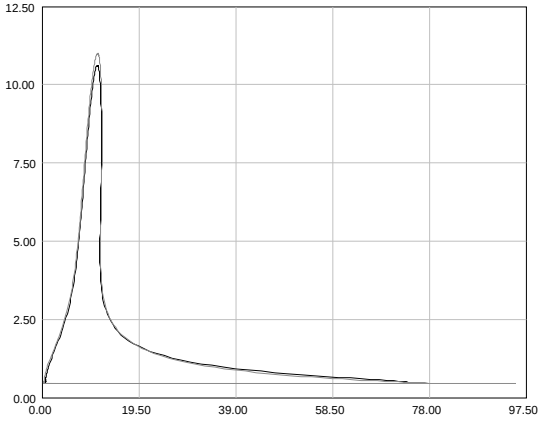

(a) Black: Rosenblatt contour, P-factor=2.75. Grey: Iso contour, P-factor=1.24.

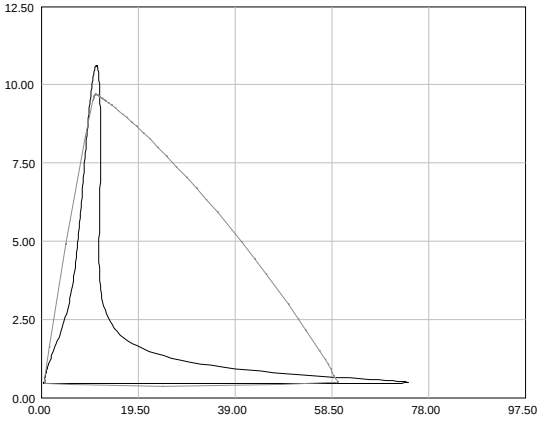

(b) Black: Rosenblatt contour, P-factor=2.75. Grey: Monte Carlo contour.

Figure 49: Northwest of Australia, total sea, 1 year return period.

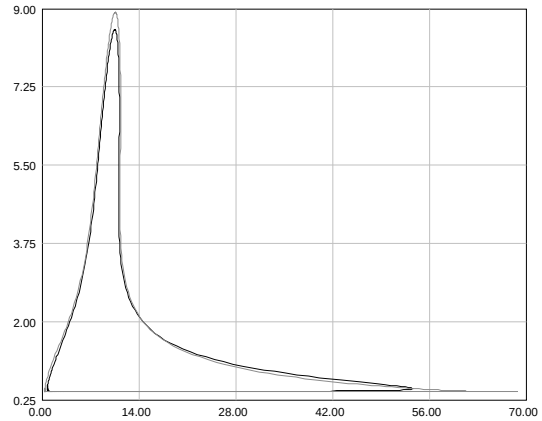

(a) Black: Rosenblatt contour, P-factor=2.72. Grey: Iso contour, P-factor=1.34.

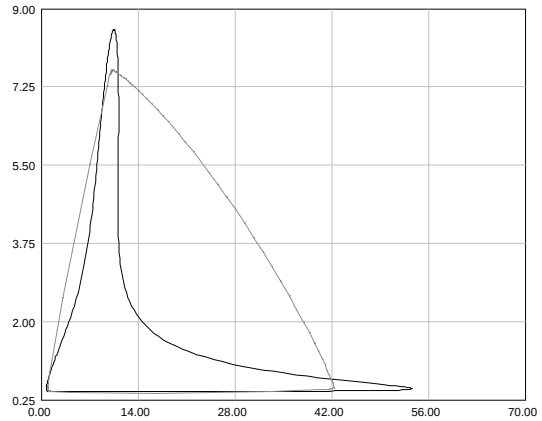

(b) Black: Rosenblatt contour, P-factor=2.72. Grey: Monte Carlo contour.

Figure 50: Northwest of Australia, total sea, 1 year return period.

For every return period for Northwest of Australia, total sea case, we observe that the adjusted Rosenblatt contour have some smaller area than the adjusted Iso contour. By comparing this with the Monte Carlo contour we see clearly that the adjusted Rosenblatt contour is still the best.

Wind sea

Table 29: Northwest of Australia, wind sea, Rosenblatt contours.

Return period	**P-factor from iterations**	**Adjusted return period**
25 years	3.26	$25 \cdot 3.26 \approx 82$ years
10 years	3.24	$10 \cdot 3.24 \approx 32$ years
1 year	3.05	$1 \cdot 3.05 \approx 3$ years

Table 30: Northwest of Australia, wind sea, Iso contours.

Return period	**P-factor from iterations**
25 years	3.47
10 years	3.15
1 year	2.23

From the tables we have the following corresponding figures:

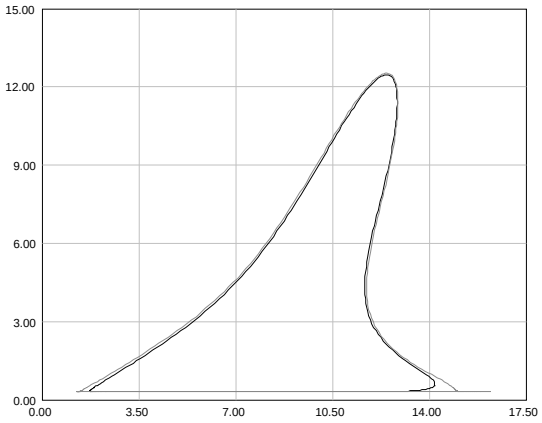

(a) Black: Rosenblatt contour, P-factor=3.26. Grey: Iso contour, P-factor=3.47.

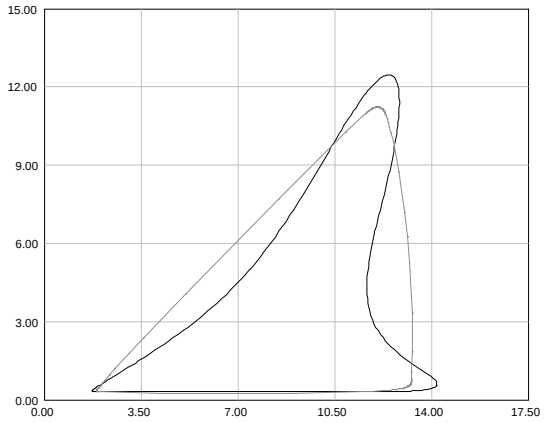

(b) Black: Rosenblatt contour, P-factor=3.26. Grey: Monte Carlo contour.

Figure 51: Northwest of Australia, wind sea, 25 years return period.

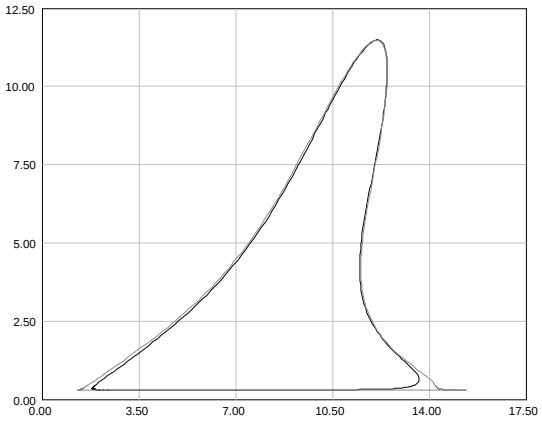

(a) Black: Rosenblatt contour, P-factor=3.24. Grey: Iso contour, P-factor=3.15.

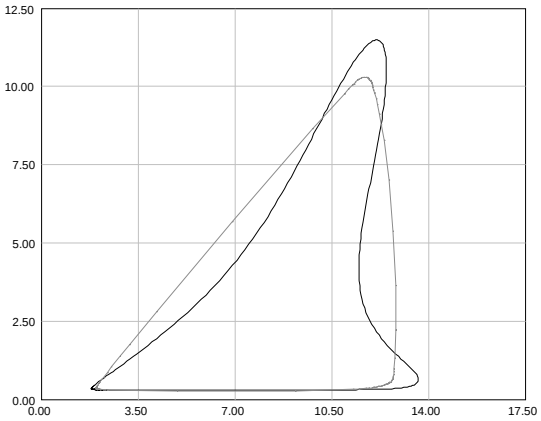

(b) Black: Rosenblatt contour, P-factor=3.24. Grey: Monte Carlo contour.

Figure 52: Northwest of Australia, wind sea, 10 years return period.

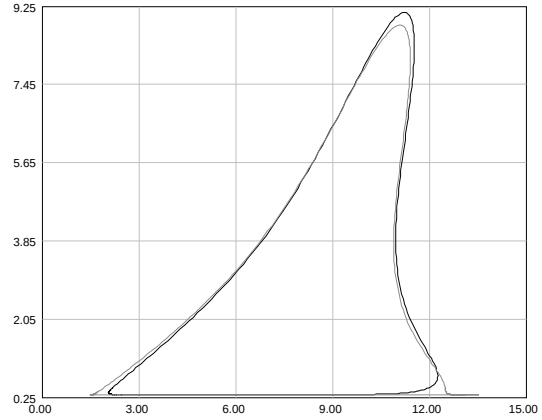

(a) Black: Rosenblatt contour, P-factor=3.05. Grey: Iso contour, P-factor=2.23.

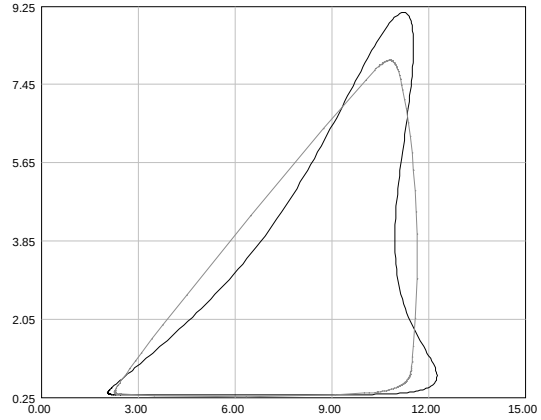

(b) Black: Rosenblatt contour, P-factor=3.05. Grey: Monte Carlo contour.

Figure 53: Northwest of Australia, wind sea, 1 year return period.

Unfortunately, for every return period for Nortwest of Australia, wind sea case, the adjusted Iso contour became numerically unstable. This is due to the vertical asymptote of the density along the line where $h = \gamma$. The instability can be seen at the lower right corner of the Iso contours. As a result the P-factor calculations are less reliable. Anyway, we observe that the adjusted Rosenblatt contour came out better than the adjusted Iso contour, so we proceed with this. Comparing the adjusted Rosenblatt contour with the Monte Carlo contour we see that the adjusted Rosenblatt contour is still the best contour.

Swell

For return periods of 25 years, 10 years and 1 year in the swell case for Northwest of Australia, we obtain 0 locally concave intervals for the Rosenblatt contours. It turns out that this is also the case for the Iso contour for a return period of 1 year. This means that the method we have used to iterate P-factors giving contours with the desired exceedance probability, will not be possible to use in these cases as we have 0 locally concave intervals to iterate from. For return periods of 25 years and 10 years for the

Iso contour, the exceedance probabilites happens to be way smaller than desired, and by changing the interval which the P-factor is varied within to $[0.5, 5]$, will not make iterations possible by the method used earlier neither. Hence, in these cases we use an alternative method for iterations of the P-factor without using concave intervals.

This alternative method iterates the P-factor by the exceedance probability evaluated using the method described in Subsection 3.1. We observe that the P-factors obtianed from this alternative iteration method in these cases are not that different from 1.0.

Table 31: Northwest of Australia, swell, Rosenblatt contours.

Return period	**P-factor from iterations**	**Adjusted return period**
25 years	1.50	$25 \cdot 1.50 \approx 38$ years
10 years	1.48	$10 \cdot 1.48 \approx 15$ years
1 year	1.40	$1 \cdot 1.40 \approx 1$ years

Table 32: Northwest of Australia, swell, Iso contours.

Return period	**P-factor from iterations**
25 years	1.15
10 years	1.14
1 year	1.13

From the tables we have the following corresponding figures:

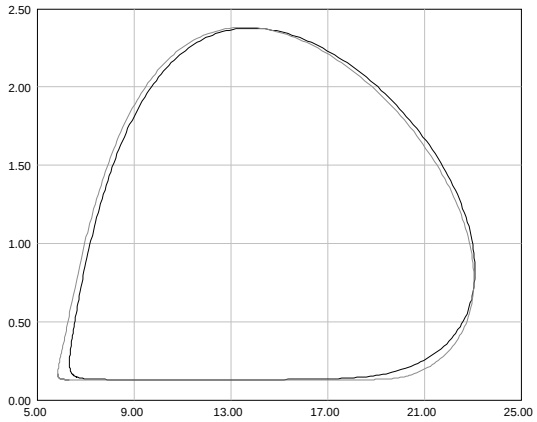

(a) Black: Rosenblatt contour, P-factor=1.50. Grey: Iso contour, P-factor=1.15.

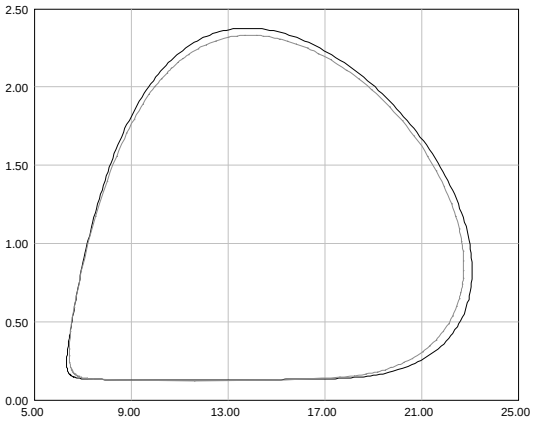

(b) Black: Rosenblatt contour, P-factor=1.50. Grey: Monte Carlo contour.

Figure 54: Northwest of Australia, swell, 25 years return period.

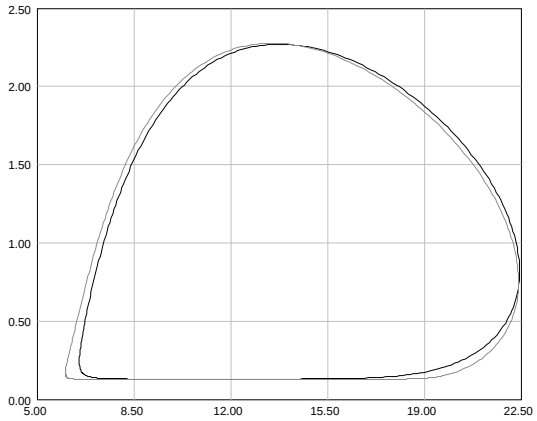

(a) Black: Rosenblatt contour, P-factor=1.48. Grey: Iso contour, P-factor=1.14.

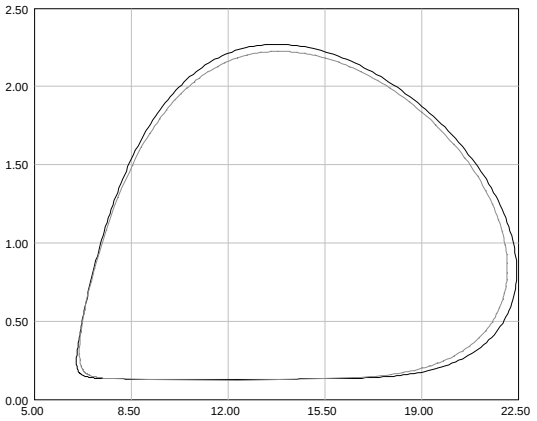

(b) Black: Rosenblatt contour, P-factor=1.48. Grey: Monte Carlo contour.

Figure 55: Northwest of Australia, swell, 10 years return period.

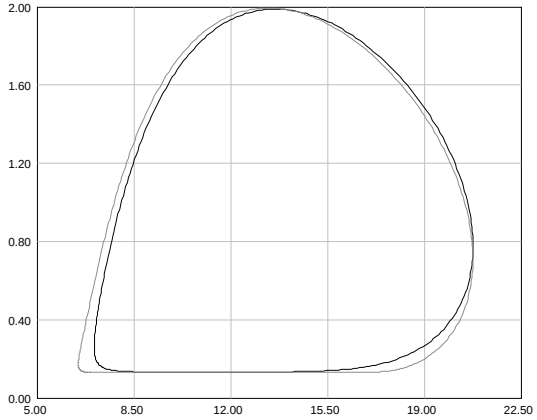

(a) Black: Rosenblatt contour, P-factor=1.40. Grey: Iso contour, P-factor=1.13.

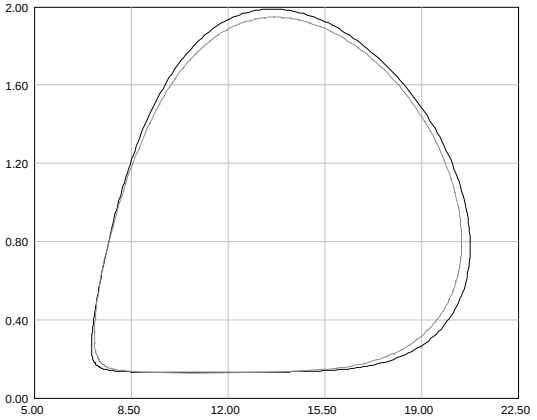

(b) Black: Rosenblatt contour, P-factor=1.40. Grey: Monte Carlo contour.

Figure 56: Northwest of Australia, swell, 1 year return period.

For every return period in the swell case for Northwest of Australia we have that the adjusted Rosenblatt contour is the best compared to the adjusted Iso contour. As we take the Monte Carlo contour into consideration we observe that this will be an even better contour.

In general, since the Iso contours in this paper are constructed such they are outside the corresponding Rosenblatt contour, we will think that the Rosenblatt contours will have the smallest area and hence are the best contours. However, summarizing the examples above, after adjusting the contours we found that this was not true in all cases. That is, the adjusted Iso contours were better than the adjusted Rosenblatt contours for West Shetland in the wind sea case, and West of Africa in the swell case.

When we in addtion to the adjusted contours included the Monte Carlo contours, we would think that this would be the best contours as these contours generally has the

desired properties. We found that this was not true in all cases neither. As we took the Monte Carlo contours into consideration, the Monte Carlo contours were only the best contours for West Shetland in the total sea case, and in the swell case, and for Northwest of Australia in the swell case.

If we summarize the best contours when all of them is taken into consideration we have that:

- The adjusted Rosenblatt contours are best for the cases: Northwest of Australia, total sea and wind sea.
- The adjusted Iso contours are best for the cases: West Shetland, wind sea, and West of Africa, swell.
- The Monte Carlo contours are best for the cases: West Shetland, total sea and swell, and Northwest of Australia, swell.

Hence, this is something to keep in mind when constructing skip designs in these areas.

When it comes to the P-factors from iterations, we had, as expected, that the P-factors for the Rosenblatt contours were higher than the corresponding P-factors for the Iso contours. The exception was for Northwest of Australia in the wind sea case for a return period of 25 years. What we also observe is that the P-factors for the Rosenblatt contours are decreasing for lower return periods. We would then think that this would also be true for the Iso contours. It turned out that the Iso contours in fact was increasing for lower return periods for West Shetland in the wind sea case, West of Africa in the swell case, and Northwest of Australia in the total sea case. However, we will not, in this paper, go into details of why it became so.

6 CONCLUSIONS

In the present paper we have introduced a precise definition of the exceedence probability of a given environmental contour with respect to a family of failure regions. We believe that this concept is needed in order to evaluate the probabilistic properties of a given contour. Throughout the numerical examples we have seen that the traditional approach based on the Rosenblatt transformation can produce a contour with an exceedence probability which is higher than desired. The alternative approach based on Monte Carlo simulation, however, is constructed so that the exceedence probability is always equal to the desired exceedance probability. On the other hand the contour based on Monte Carlo simulation can sometimes be too conservative and include areas with very low probability when the joint distribution of the environmental variables are concentrated in a non-convex region.

For Monte Carlo simulations we showed techniques for how to identify the boundary of the set $\mathcal{B}$, i.e., $\partial\mathcal{B}$ using estimates of $C(\theta)$ and estimates of its derivative. We explained an importance sampling method which only focuses on the estimation on the area of interest. This reduces the number of simulation which might be large when P_e is very small. Avoiding small irregularitites on the estimated contour from the suggested Monte Carlo method, we used the boundary of the convex hull of all estimated points along the contour instead of the original polygon, resulting in smoother contours.

As the Rosenblatt contours can sometimes be overly conservative in some areas, it was interesting to also include a third type of environmental contours, the Iso contours. We then had three types of environmental contours to compare; the Rosenblatt contours, the Monte carlo contours and the Iso contours. For the Rosenblatt contours and the Iso contours we used P-factors from itereation to adjust the contours such that they got the desired exceedance probability. Hence, when all the contours had the same desired exceedance probability, we were able to compare them graphically and could find which contour had the lowest area and hence was the best. Knowing that the contour with the lowest area is the best makes it easier to choose the best contour for the given application.

References

[BHØ10] Gro Sagli Baarholm, Sverre Haver, and Ole David Økland. "Combining contours of significant wave height and peak period with platform response distributions for predicting design response". In: *Marine Structures* 23.2 (2010), pp. 147–163.

[BF85] Richard L Burden and J Douglas Faires. "2.1 The bisection algorithm". In: *Numerical Analysis. Prindle, Weber & Schmidt, Boston, MA., pp. x* 676 (1985).

[Dit02] Ove Ditlevsen. "Stochastic model for joint wave and wind loads on offshore structures". In: *Structural Safety* 24.2 (2002), pp. 139–163.

[Fon+13] E Fontaine et al. "Reliability analysis and Response Based Design of a moored FPSO in West Africa". In: *Structural Safety* 41 (2013), pp. 82–96.

[Gra72] Ronald L. Graham. "An efficient algorith for determining the convex hull of a finite planar set". In: *Information processing letters* 1.4 (1972), pp. 132–133.

[Has+17] Andreas F Haselsteiner et al. "Deriving environmental contours from highest density regions". In: *arXiv preprint arXiv:1701.02666* (2017).

[Hav87] Sverre Haver. "On the joint distribution of heights and periods of sea waves". In: *Ocean Engineering* 14.5 (1987), pp. 359–376.

[HW09] Sverre Haver and Steven R Winterstein. "Environmental contour lines: A method for estimating long term extremes by a short term analysis". In: *Transactions of the Society of Naval Architects and Marine Engineers* 116 (2009), pp. 116–127.

[HVN15a] Arne B Huseby, Erik Vanem, and Bent Natvig. "A new Monte Carlo method for environmental contour estimation". In: *Safety and Reliability : Methodology and Applications. Proceedings of the European Safety and Reliability Conference (ESREL)*. 2015, pp. 2091–2098.

[HVN13] Arne Bang Huseby, Erik Vanem, and Bent Natvig. "A new approach to environmental contours for ocean engineering applications based on direct Monte Carlo simulations". In: *Ocean Engineering* 60 (2013), pp. 124–135.

[HVN15b] Arne Bang Huseby, Erik Vanem, and Bent Natvig. "Alternative environmental contours for structural reliability analysis". In: *Structural Safety* 54 (2015), pp. 32–45.

[JEF11] Philip Jonathan, Kevin Ewans, and Jan Flynn. "On the Estimation of Ocean Engineering Design Contours". In: *ASME 2011 30th International Conference on Ocean, Offshore and Arctic Engineering*. American Society of Mechanical Engineers. 2011, pp. 695–705.

[Moa09] Torgeir Moan. "Development of accidental collapse limit state criteria for offshore structures". In: *Structural Safety* 31.2 (2009), pp. 124–135.

[oRo98] Joseph o'Rourke. *Computational geometry in C*. Cambridge university press, 1998.

[Ros52] Murray Rosenblatt. "Remarks on a multivariate transformation". In: *The annals of mathematical statistics* 23.3 (1952), pp. 470–472.

[VB12] Erik Vanem and Elzbieta M Bitner-Gregersen. "Stochastic modelling of long-term trends in the wave climate and its potential impact on ship structural loads". In: *Applied Ocean Research* 37 (2012), pp. 235–248.

[VB15] Erik Vanem and Elzbieta M Bitner-Gregersen. "Alternative Environmental Contours for Marine Structural Design—A Comparison Study". In: *Journal of Offshore Mechanics and Arctic Engineering* 137.5 (2015).

[Win+93] Steven R Winterstein et al. "Environmental parameters for extreme response: Inverse FORM with omission factors". In: *Proceedings of the ICOSSAR-93, Innsbruck, Austria* (1993).